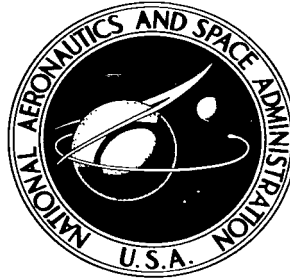


NASA TECHNICAL NOTE

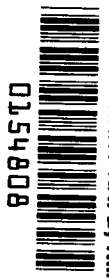


NASA TN D-2231

2.1

NASA TN D-2231

LOAN COPY:  
AFWL (KIRTLAND AFB)



TECH LIBRARY KAFB, NM  
TO

A FLIGHT INVESTIGATION OF THE  
PERFORMANCE, HANDLING QUALITIES,  
AND OPERATIONAL CHARACTERISTICS  
OF A DEFLECTED SLIPSTREAM STOL  
TRANSPORT AIRPLANE HAVING  
FOUR INTERCONNECTED PROPELLERS

*by Hervey C. Quigley, Robert C. Innis,  
and Curt A. Holzhauser*

*Ames Research Center  
Moffett Field, California*

TECH LIBRARY KAFB, NM  
  
0154808

A FLIGHT INVESTIGATION OF THE PERFORMANCE, HANDLING QUALITIES,  
AND OPERATIONAL CHARACTERISTICS OF A DEFLECTED SLIPSTREAM  
STOL TRANSPORT AIRPLANE HAVING FOUR  
INTERCONNECTED PROPELLERS

By Hervey C. Quigley, Robert C. Innis,  
and Curt A. Holzhauser

Ames Research Center  
Moffett Field, Calif.

NATIONAL AERONAUTICS AND SPACE ADMINISTRATION

For sale by the Office of Technical Services, Department of Commerce,  
Washington, D.C. 20230 -- Price \$1.50

A FLIGHT INVESTIGATION OF THE PERFORMANCE, HANDLING QUALITIES,  
AND OPERATIONAL CHARACTERISTICS OF A DEFLECTED SLIPSTREAM  
STOL TRANSPORT AIRPLANE HAVING FOUR  
INTERCONNECTED PROPELLERS

By Hervey C. Quigley, Robert C. Innis,  
and Curt A. Holzhauser

Ames Research Center  
Moffett Field, Calif.

SUMMARY

A large four-engined aircraft having full-span triple-slotted, trailing-edge flaps and interconnected propellers was studied to gain further information on the flight and operational characteristics of typical STOL aircraft. The airplane investigated - the Breguet 941 - had good STOL performance with the capability of making a landing approach with a glide slope of about  $8^{\circ}$  at an airspeed of less than 60 knots. The take-off and landing distances over 35 and 50 feet obstacles, respectively, were less than 1000 feet. The STOL handling qualities of the airplane were rated satisfactory except for longitudinal static stability and the lateral-directional static and dynamic stability which were rated acceptable. Because of a propeller interconnect feature the airplane was considered safe to fly at the low airspeeds required for STOL performance.

INTRODUCTION

The interest in STOL transport airplanes for military transport missions and for short-haul airlines has created a requirement for information on the performance, handling qualities, and operational characteristics of deflected slipstream airplanes. The principle of obtaining augmented lift by deflecting the propeller slipstream with highly deflected trailing-edge flaps has been demonstrated in flight on several airplanes. In this country, limited experience has been obtained by flying the YC-134A, NC-130B, and VZ-3 STOL vehicles. The results of these investigations have been reported in references 1 through 4. In France an extensive research and development program has been carried out on the deflected slipstream STOL transport airplanes by the Breguet Aircraft Company. As noted in references 5 and 6, initial studies on the Breguet 94 series date back to 1945 and the first flight on the Breguet 940 test vehicle was made in 1957. The Breguet 940 demonstrated experimentally the feasibility of the highly deflected triple-slotted flap, interconnected propellers, and the use of differential outboard propeller pitch for control to obtain acceptable STOL performance and handling qualities. These features were then incorporated into a prototype assault transport known as the Breguet 941. Reference 5 describes some of the performance and handling qualities characteristics of the 941 aircraft in STOL operation.

In order to gain additional information on the operation of large STOL aircraft, the NASA has conducted an investigation of the Breguet 941 airplane, including a limited flight study in France in cooperation with the French Air Force and the Societe Anonymes des Ateliers D'Aviation, Louis Breguet. The results of the investigation are presented herein as representative of the characteristics of a current state-of-the-art design. Some of the basic aircraft flight test data on which the report is based as received from Breguet without analysis are available from Ames Research Center upon request.

#### NOTATION

$A_x$	longitudinal acceleration, ft/sec <sup>2</sup> /g
$A_z$	normal acceleration, ft/sec <sup>2</sup> /g
$\bar{C}_D$	drag coefficient including thrust
$C_L$	lift coefficient, $\frac{A_z W}{q_\infty S}$
$C_{L_{max}}$	maximum lift coefficient
$C_m$	pitching-moment coefficient
$C_{m_\alpha}$	longitudinal stability derivative, $\frac{\partial C_m}{\partial \alpha}$ , per radian
$C_{m_v}$	longitudinal stability derivative, $\frac{\partial C_m}{\partial V}$ , per ft/sec
$g$	acceleration of gravity, ft/sec <sup>2</sup>
$i_t$	horizontal stabilizer angle (leading edge up, positive), deg
$N_g$	gas generator speed, percent
$p$	roll angular velocity (right roll, positive), radians/sec
$q$	pitch angular velocity (nose-up, positive), radians/sec
$q_\infty$	free-stream dynamic pressure, lb/ft <sup>2</sup>
$\frac{R}{C}$	rate of climb, ft/min
$\frac{R}{S}$	rate of descent, ft/min
$r$	yaw angular velocity (nose right, positive), radians/sec
$S$	wing area, ft <sup>2</sup>
$SHP$	shaft horsepower

T	propeller thrust, lb
T <sub>0</sub>	static propeller thrust, lb
T <sub>C</sub>	thrust coefficient, $\frac{T}{qS}$
V	true airspeed, knots or ft/sec
V <sub>C</sub>	calibrated airspeed, $V\sqrt{\sigma}$ , knots
V <sub>S</sub>	stall or minimum airspeed, knots
W	gross weight, lb
$\alpha$	corrected angle of attack, deg
$\alpha_u$	indicated angle of attack, deg
$\beta$	angle of sideslip, deg
$\gamma$	flight-path angle (climb, positive), deg
$\delta_e$	elevator angle (trailing edge down, positive), deg
$\delta_f$	trailing-edge flap deflection, deg
$\delta_r$	rudder deflection (trailing edge left, positive), deg
$\delta_s$	lateral stick deflection, deg
$\eta$	propeller efficiency
$\theta$	attitude angle (nose up, positive), deg
$\sigma$	density ratio
$\phi$	bank angle (right wing down, positive), deg
$\ddot{\phi}$	roll angular acceleration, radians/sec <sup>2</sup>

#### DESCRIPTION OF AIRPLANE

The test airplane, a high-wing, turboprop, assault transport airplane, is shown in figure 1 in the landing configuration. A three-view sketch of the airplane is shown in figure 2, and the pertinent geometric data are presented in table I. The airplane has several unique features: (1) most of the wing is immersed in the propeller slipstream, and it is equipped with a highly deflected, full-span, triple-slotted trailing-edge flap and a cambered leading edge, (2) the four propellers are interconnected by a cross shaft and have opposite rotation; that is, the left inboard and right outboard turn clockwise and the left outboard

and right inboard turn counterclockwise (see fig. 2), (3) differential outboard propeller pitch is used to augment lateral and directional control, and (4) the cockpit controls included a pilot's stick for lateral and elevator control and a single throttle at the pilot's left hand for all four engines.

### Trailing-Edge Flaps

Figure 3 presents a sketch of the trailing-edge flaps. The flap chord is 38.5 percent of the wing chord and is constructed with three chordwise sections. The angle between the lower, or trailing edge, section and the normal wing chord line defines the flap deflection. The small middle surface is rigidly attached to the lower flap section. The upper flap section is deflected about one-half that of the lower section.

The flap is divided into four spanwise sections on each wing. The two inboard sections are known as the internal flap and the two outboard sections as the external flap. The aft section of the external flap serves as an aileron. The deflections for the four flap configurations tested and the notation used in this report to identify the flap configurations are as follows:

Configuration	Internal	External	Notation
Cruise	0	0	0/0
Take-off	45°	30°	45/30
Wave-off	75°	50°	75/50
Landing	98°	65°	98/65

### Flight Controls

A short control stick, about 8 inches long, on top of the control column is used to control the airplane laterally. The control stick operates ailerons, spoiler, and differential outboard propeller pitch to produce lateral control moments. Figure 4 shows the variation of the flight control displacements with pilot's control displacement for all the controls. As shown in figure 4(a), the spoilers have been rigged slightly up on both wings which reduces the nonlinear effectiveness associated with spoiler deflection near zero deflection.

Standard rudder pedals are used to operate the double-hinged rudder and differential propeller pitch for directional control. The double-hinged rudder consists of two chordwise surfaces of about equal chords (see fig. 1). The forward surface has half the deflection of the aft surface. At airspeeds above 100 knots, the forward rudder is locked at zero deflection and only the aft surface is used and can be deflected  $\pm 40^\circ$ . The variation of differential propeller pitch with both lateral and directional control is shown in figure 4(b).

Longitudinal control was provided by the control column pivoted from the floor. An adjustable horizontal stabilizer was normally set at +3 for take-off, at +9 for landing, and at +1 for cruise.

The ailerons, spoilers, elevators, and rudder are actuated by an irreversible hydraulic control system with control forces supplied by feel springs. The control force variation with pilot's control displacement is shown in figure 5; the breakout forces and friction are also shown by these data. The differential outboard propeller pitch is actuated by a mechanical mixing system from the lateral control stick and rudder pedals to the propeller pitch control system. The horizontal stabilizer is actuated by the hydraulic system but is controlled electrically.

### Propulsion System

Power is supplied by four gas turbine engines each with a power rating of 1165 horsepower. The engines are coupled to the cross shaft through a gear train and a free-wheeling unit. Each propeller is coupled to the cross shaft through a gear box and a clutch. The maximum speed of the cross shaft is 6000 rpm. The estimated losses due to gearing and accessories are 25 horsepower per engine. Each of the four propellers has three blades, 14.76 feet in diameter, with a maximum speed of 1200 rpm. Propeller characteristics used to compute the thrust coefficients are based on 0.55-scale propeller tests performed in a 26-foot wind tunnel of ONERA. These tests showed that the static propeller performance was 4.2 pounds of thrust per shaft horsepower (figure of merit equal to 0.57) at 1100 horsepower and the cruise efficiency was 82 percent.

The shaft and, therefore, the propeller speed is controlled by a governor which adjusts the pitch of all four propellers simultaneously. This shaft speed is set by a lever in the cockpit. The power output of each engine is determined by its gas generator speed which can be adjusted by individual engine throttles on the center pedestal in the cockpit. Further, the gas generator speed of all engines can be collectively controlled by a single power lever to the left of the pilot. This lever moves all four throttles together. Also incorporated into the single-power control lever was the control for propeller reverse pitch. It was possible to put the propeller into reverse from any throttle position. This was accomplished without unloading the engines by having the inboard propeller pitch lead the outboard propeller pitch when going to reverse pitch. There were several safety features on this control to prevent the pilot from inadvertently placing the control in reverse pitch during flight.

### Instrumentation

All quantities were recorded by oscillographs. Take-off and landing distances were measured by the use of a phototheodolite and direct ground measurements.

Special cockpit instrumentation included angle of attack and sideslip indicators. A paravisual angle-of-attack indicator (BIP) was also provided. This instrument consisted of three lights mounted above the instrument panel in the view of the pilot as he looked out of the windshield of the airplane. The lights were controlled by angle of attack. A green light indicated an angle of attack between  $0^{\circ}$  and  $+3^{\circ}$ . Amber plus green indicated an angle of attack less than  $0^{\circ}$  while red plus green indicated an angle of attack greater than  $+3^{\circ}$ . Red alone indicated an angle of attack above  $13^{\circ}$ . A stick shaker was also operated by this system to provide stall warning.

### Test Procedures and Conditions

The tests were conducted at Centre D'Essais en Vol (French Flight Test Center) at Istres, France under VFR flight conditions. The flights were made by an NASA pilot in cooperation with Breguet personnel and with a Breguet test pilot and/or flight test engineer aboard. All NASA landings and take-offs were from a concrete field at an elevation of 82 feet. A landing approach mirror was used for a portion of the landing evaluation.

The airplane was flown with a take-off gross weight of 38,600 pounds with the center of gravity at 30.8 percent of MAC. The loading consisted of the test instrumentation, water ballast, and 3,200 liters (about 5,500 pounds) of fuel. Final landing gross weight was about 36,000 pounds with little change in center-of-gravity position from take-off to landing.

### RESULTS AND DISCUSSION

The results of the investigation will be discussed in three sections entitled (1) Performance, (2) Handling Qualities, and (3) Operational Techniques. The lift and drag characteristics are presented in the appendix.

#### Performance

The take-off, landing, and cruise performance for the test airplane are summarized in the following table for a gross weight of 38,500 pounds. All of the values listed are based on measurements made during Breguet and NASA flights.

Take-off ( $\delta_F = 45/30$ )

	Flight idle	3 engine	4 engine
Power	4 - 200 SHP	3 - 1100 SHP	4 - 1100 SHP
Stall speed, knots	68	53	49
Take-off speed, knots	-	-	59
Ground roll on concrete, ft	-	-	450
Air distance to 35 ft, ft	-	-	450
Total distance to 35 ft, ft	-	-	900

Landing ( $\delta_F = 98/65$ )

	Flight idle	$\gamma = -7.5^\circ$	$\gamma = -5.0^\circ$
Power (each of 4 engines)	~200 SHP	330 SHP	520 SHP
Stall speed, knots	60	55	49
Approach speed, knots	-	61	57
Air distance, ft	-	350	600
Ground roll on concrete or grass, ft	-	300	250
Total distance over 50 ft, ft	-	650	850

Cruise ( $\delta_F = 0/0$ )

Altitude, ft	0	10,000
Normal continuous power (each of four engines)	1100 SHP	900 SHP
True airspeed, knots	225	225

Take-off. - The effect of gross weight on the measured ground roll and total distance over 35 feet is shown in figure 6 for take-offs on grass and concrete. Data are shown for flights made by Breguet and NASA; data obtained by Centre D'Essais en Vol were used in establishing the faired average curve. These data are for the normal take-off configuration with an average power of 1100 horsepower per engine. The operational envelope for the airplane in the take-off configuration is presented in figure 7. These data show the climb-out angle variation with airspeed as well as the angle of attack required for various airspeeds. An angle of attack of about  $10^\circ$  is required for a lift-off speed of 59 knots. The procedure used in the take-off maneuver is illustrated by figure 8 which shows a time history of a typical take-off. It can be seen that shortly after lift-off the angle of attack is reduced as airspeed increases. Although this procedure did not take complete advantage of the STOL take-off capability of the airplane, the pilots considered it an easy and safe technique. (Further discussion of the take-off procedure is included in the Operational Techniques

section of this report.) Calculations have shown that air distance could be reduced if higher angles of attack were maintained during transition thereby utilizing the available energy to increase altitude instead of increasing airspeed so rapidly.

Landing.- The variation of the computed landing distances with gross weight is shown in figure 9. Spotted on the curves are the measured ground-roll distances and distances over 50 feet obtained during Breguet and NASA tests. Data are shown for descent angles of  $5^{\circ}$  and  $7.5^{\circ}$  representing the operational range of approach angles. The landing distances over 50 feet are less than 1,000 feet for the maximum landing weight considered for the airplane. The operational envelope for the landing configuration is shown in figure 10 with pilots' approach speeds marked at various descent angles. Approaches were generally made at an indicated angle of attack of about  $3^{\circ}$  with engine power set for the desired descent angle. For a gross weight of 38,500 pounds and at  $3^{\circ}$  angle of attack the approach speed was approximately 57 knots for a  $5^{\circ}$  descent angle and 61 knots for  $7.5^{\circ}$ . These approach conditions gave a  $12^{\circ}$  indicated angle-of-attack margin and about a 7-knot air-speed margin from the stall. The landing procedure was to make only a half-flare, that is, with a rate of sink at touchdown, and reversing the pitch of the propellers immediately at touchdown. A time history of a typical landing is shown in figure 11. The "half-flare" technique of landing will be discussed in more detail in the Operational Techniques section of the report. With this technique it was not considered necessary to increase the airspeed margin (decrease angle of attack) as the descent angle became steeper. In contrast, a significant increase in the airspeed margin was necessitated in the tests reported in references 1 and 2 to avoid stalling when full flares were used. Figure 12 shows that with the half-flare technique, the calculated ground distance varied only a small amount with descent angle because touchdown speed was nearly constant. Therefore, the total landing distance over an obstacle depends primarily on the air distance which is a function of the descent angle. It can be noted that as the descent angle was increased to more than  $8^{\circ}$ , the change in total landing distance per degree of descent angle was small. The landing distances during NASA flights were longer than Breguet's because the pilots' lack of familiarity with the propeller reverse pitch mechanism caused a delay of 1 to 2 seconds in application of reverse thrust.

All landing data presented herein were without "transparency." ("Transparency" is the term used in reference 6 to describe the approach power condition when the outboard propellers are at zero equivalent thrust and the inboard propellers are developing the thrust required.) Based on the Breguet 940 flight work described in reference 6, improvement in the landing performance may be possible on the test airplane and other similar STOL aircraft if transparency is used.

Wave-off.- Because of the high drag in the landing configuration, the wave-off required a reduction in flap deflection from 98/65 to 75/50. Figure 13 compares the STOL operational envelopes of the airplane in the landing configuration and the wave-off configuration. The data indicate the wave-off capability in the landing configuration would be adequate only with four engines. It can be seen that if the flaps are retracted from 98/65 to 75/50 at an airspeed of 60 knots with maximum power on three engines, the rate of climb increases from 60 to

450 feet per minute. The stall speeds for the two configurations are nearly the same ( $\approx 43$  knots), indicating that there is little difference in the lift characteristics with the two flap deflections, but a large effect on drag. (See appendix for lift and drag characteristics.)

Cruise.- Figure 14 presents curves of power required and power available for several altitudes and gross weights. These data indicate that with the current propulsion system, which has a maximum propeller efficiency of about 82 percent, cruise speeds of 225 knots true airspeed are obtained at sea level and 10,000 feet altitude with maximum continuous engine power. The beneficial effects of altitude on the drag-airspeed relationship was compensated by the loss of engine power with altitude. The lift-to-drag ratio of this airplane at 10,000 feet altitude and 225 knots true airspeed is about 9.5.

### HANDLING QUALITIES

The handling qualities of the test airplane in the STOL operating range were considered satisfactory by the evaluating pilot except for the longitudinal static stability and lateral-directional static and dynamic stability which were unsatisfactory but acceptable. Analysis of the measured characteristics has been made to show the relationship to pilot opinion. The numerical pilot rating system shown in table II and described in reference 8 was used by the pilot in rating the various characteristics.

#### General Control Characteristics

The control characteristics about all three axes of the airplane in the normal landing configuration at about 60 knots airspeed along with the pilot ratings are shown in the following table. The control power is in terms of initial angular acceleration for full control. The sensitivity is in terms of initial angular acceleration for 1 inch of control deflection. The damping is in terms of damping moment divided by moment of inertia per radian per second angular velocity. The response is in terms of degrees after one second for a 0.2-second-ramp<sup>1</sup> maximum control step input, and for computing purposes a first-order system was assumed.

Axes	Control power, radians/sec <sup>2</sup>	Sensitivity, radians/sec <sup>2</sup> /in.	Damping, 1/sec	Response after 1 sec, deg	Pilot's rating
Lateral	0.42	0.14	1.0	7.5	3
Directional	.18	.06	.15	3.5	3
Longitudinal	1.05	.15	2	14	3-1/2

<sup>1</sup>The ramp time is the time assumed for the controls to reach maximum displacement.

These data show that the pilot rated the STOL control response characteristics "satisfactory" about all three axes. The rigging of the spoilers so that maximum deflection occurred at half stick deflection, as shown in figure 4(a), was responsible for the high lateral control sensitivity. The resulting non-linearity was considered to be satisfactory by the pilot.

At minimum airspeeds (as low as 42.5 knots), the pilot considered control to still be adequate for this class of airplane. In the take-off configuration the longitudinal and directional control were not appreciably different than in the landing configuration, but the lateral control was rated higher (pilot rating of 2-1/2). Measurements showed that lateral control response was higher in the take-off configuration because the ailerons were more effective at a reduced angle of droop.

In the cruise configuration lateral and directional control were considered to be too sensitive for this type of airplane; longitudinal control was much too sensitive with a pilot rating of 6. A control feel system which varies with free-stream dynamic pressure is planned for future aircraft to minimize this problem.

Because of the desirability of flying with one hand on the throttle and the other on the flight controls, the pilots found the left-hand throttle control and the right-hand stick control for lateral and longitudinal control inputs very convenient. The break-out forces and friction were low about all three axes (see fig. 5). The force gradients shown in figure 5 were felt to be satisfactory for STOL operation, but directionally and longitudinally were too low for cruise. The control force characteristics of the left-hand throttle consisted of a fairly high break-out force due to a detent system but with very little force once the throttle lever was moving. Therefore, it was difficult for the pilot to make small throttle movement without overcontrolling. It is believed that a desirable force characteristic of the throttle system for a STOL airplane would be just enough friction to prevent creep.

#### Lateral Control

Since lateral control requirements for STOL operation are of such general interest, several lateral configurations were evaluated. The normal configuration uses ailerons, spoilers, and differential propeller pitch to produce rolling moment with lateral stick inputs. It was also possible to disengage each of them. Figure 15 presents the rolling angular acceleration with lateral stick deflection for several configurations. The lateral control characteristics of all combinations tested are summarized along with the pilot rating of each in table III.

These data show that disengaging the spoilers reduces lateral control power in the landing configuration from 0.42 to 0.17 radian/sec<sup>2</sup> and the sensitivity to 0.03 radian/sec<sup>2</sup> per inch of stick deflection. The pilot did not consider this a safe configuration, hence, the rating of 7-1/2. With the differential propeller pitch disengaged and with the spoilers and aileron operating, the

control power was reduced to 0.30 radian/sec<sup>2</sup> and the pilot rating was 5. The pilot's comments on this configuration stated that the lateral control response and adverse yaw characteristics felt quite similar to the NC-130B STOL aircraft (ref. 2). The relatively large adverse yaw which occurred without differential propeller pitch was very objectionable. The large adverse yaw resulted from the deflection of the drooped outboard flaps acting as ailerons. Breguet wind-tunnel data show that the spoiler also contributes to the adverse yaw. Therefore, the differential propeller pitch on the 941 contributes in two important ways to lateral control of the airplane; first, by an increase in control power, and second, by reduced adverse yaw.

When the ailerons were locked, lateral control moments were produced by spoilers and differential propeller pitch. Without aileron, the roll control power was reduced only about 10 percent, and the adverse yaw disappeared and was replaced by a favorable yaw characteristic. The pilot considered the lateral control in this configuration satisfactory. The favorable yaw was satisfactory in STOL operation, but was excessive during cruise because it was difficult to prevent large sideslip angles from building up during turn entries. When the differential propeller pitch was disengaged in cruising flight, leaving only the spoilers for lateral control, the pilot considered the lateral control very good (rating of 2). The spoiler only configuration was not evaluated in STOL operation.

Subsequent to this investigation, the configuration of the airplane was changed by eliminating the aileron and deflecting the outboard flap to higher angles. To obtain higher lateral control power without the aileron, the spoilers were made more effective and the differential propeller pitch was increased to 3.5°. With these modifications the control power in take-off was increased from 0.44 to 0.60 radian/sec<sup>2</sup> and the control power in landing was increased from 0.40 to 0.70 radian/sec<sup>2</sup>. The NASA evaluating pilot found that the modified airplane was more responsive to lateral control inputs and could roll to about 10° in one second in the landing configuration. The pilot rated the modified lateral control satisfactory for both taking off and landing.

Figure 16 presents the variation of lateral control power with pilot's rating for the various configurations of the Breguet airplane. The control power and pilot's rating of the VZ-3RY, YC-134A, and NC-130B STOL airplanes are shown for comparison. Although these data indicate little improvement in pilot rating for control powers greater than 0.4 radian/sec<sup>2</sup>, more data are needed to adequately define a satisfactory control power level because adverse yaw and other characteristics undoubtedly have a strong influence on the pilot's rating of lateral control in STOL operation.

### Static Lateral and Directional Stability

The static lateral and directional stability characteristics are shown in figure 17 in terms of lateral stick and rudder pedal position and bank angle variation with sideslip angle in the landing configuration. The static directional

stability was positive. The rudder pedal position variation with sideslip out to at least  $20^\circ$  of sideslip was linear; the airplane has been flown to as high as  $30^\circ$  of sideslip without any divergence apparent to the pilot. The pilots considered the static directional stability low, with a pilot rating of 4.

The dihedral effect which is indicated by the lateral stick required for steady-state sideslip was positive but low. The nonlinearity in the lateral stick position variation with sideslip is believed due to nonlinearity in the lateral control effectiveness and not in the dihedral effect. It should be pointed out, however, that the pilot was unaware of any nonlinearity in lateral response near zero stick deflection. The control system of the airplane was such that the rudder pedal also produced some differential propeller pitch (see fig. 4(b)). This was incorporated to increase the rolling moment with rudder deflection to synthesize a dihedral effect. The pilot considered the dihedral effect satisfactory.

As expected with opposite rotating propellers, there were no appreciable lateral or directional trim requirements due to speed or angle-of-attack changes.

#### Lateral-Directional Dynamic Stability

At the normal approach speed, the directional oscillation has a period of 8.5 seconds and a damping ratio less than 0.1. Figure 18 is a time history of the lateral-directional oscillation following a release from steady-state sideslip, and figure 19 is a time history of the response of the airplane to a lateral stick pulse input (bank angle step) with rudder fixed. These two time histories show the characteristic behavior of an airplane with low directional stability, low side-force gradient, and low damping. Large amplitude and long period sideslip and yaw rate oscillations are evident, and for rudder-fixed rolls large sideslip angles build up before the airplane begins to turn when the airplane is banked. Although the airplane had similar lateral-directional dynamic characteristics to the NC-130B (refs. 2 and 3), the pilot considered the test airplane to be acceptable and assigned a rating of 4, as compared to a pilot rating of 6-1/2 for the NC-130B. An analysis of the differences in the characteristics of the two airplanes failed to show that any one parameter could account for the large difference in pilot opinion. The shorter period of 8.5 seconds for the test airplane, as compared to 12 seconds for the NC-130B, was probably an important factor. Also the lateral control power was 20 percent higher for the 941, adverse yaw was close to zero, there was no tendency for divergence in sideslip at high sideslip angles, and the mechanical characteristics of the control system were considered to be much better. It seems reasonable that the combination of all these characteristics could account for the difference in pilot opinion.

#### Static Longitudinal Stability

The evaluating pilot considered the static longitudinal stability of the airplane low in all configurations and airspeeds. Stabilizing on a desired angle

of attack was no problem for the pilot in calm air, but in turbulent air, the pilot found it difficult to keep angle-of-attack excursions low. The numerical pilot ratings were 4-1/2 in STOL operation and 5-1/2 in cruise.

Figure 20 presents the longitudinal stability characteristics of the airplane in terms of elevator angle variation with angle of attack for three engine powers and a center of gravity of 32-percent MAC. These data show that the elevator required for trim varies with power setting. Not only is a trim change with thrust evident, but also a change in slope. An analysis has indicated that the moment change associated with changes in thrust coefficient as airspeed is changed has a strong effect on the longitudinal stability. These characteristics are discussed in more detail in reference 7. This reference points out that the effect of thrust-coefficient changes on the static longitudinal stability are a function of the vertical center-of-gravity position. Also evident in figure 20 is the change in the slope of the curve at high angles of attack. The change in slope probably results from a change in downwash characteristics at the tail at high angles of attack. A discussion of the downwash characteristics on a model similar to the Breguet 941 is given in reference 9.

Figure 21(a) shows the elevator position variation with angle of attack for various center-of-gravity positions in the landing configuration. These data show that with the center of gravity at 35-percent MAC the stability is almost neutral, while near 30-percent MAC the stability is positive. The longitudinal-stability data for the center of gravity at 30.8-percent MAC used in the NASA evaluation flights are shown in figure 21(b).

The static longitudinal stability in the cruise configuration was almost neutral at a center-of-gravity location of 30.8-percent MAC. Less than 1° of elevator deflection was required for the airspeed range from 160 to 230 knots indicated airspeed (about 3-1/2° angle-of-attack change). The pilot found that the low stability was not too annoying for test flying, but it would be unsatisfactory for a long flight, hence, a pilot rating of 5-1/2.

#### Trim Changes With Flap Deflection and Engine Power

Figure 20 also shows the static longitudinal characteristics at various engine power and flap settings. These data can indicate trim change with engine power, but they do not give an exact indication of the trim change with flap deflection since the stabilizer angle is different for each flap deflection. The recommended operational procedure was to change stabilizer trim as flap deflection was changed. The stick forces were unacceptably high when going from either take-off or landing configuration to flap-up or vice-versa without changing stabilizer position. For example, a pull force of the order of 15 pounds was required for a constant stabilizer angle transition from take-off configuration at an airspeed of 65 knots to cruise configuration at an airspeed of 130 knots.

Figure 20 indicates that there is a large nose-down trim moment with an increase in engine power. Because of this large trim change with thrust, the airplane was equipped with a trim compensator which operated on the elevator trim

bungee and varied the elevator position for zero stick force as a function of throttle position. The pilot considered this method of compensating for the trim change with power to be quite satisfactory. The throttle-elevator force interconnect was particularly helpful in wave-offs. Figure 22 shows time histories with and without the compensator. These data of simulated wave-offs were made stick-free. It can be seen that, with the interconnect, successful wave-off can be accomplished without change in trim force. Going from 90 percent of maximum gas generator speed to 100 percent resulted in the elevator position for zero force of  $-4^{\circ}$ . The pilot liked the positive nose-up rotation with increase in thrust evident with the interconnect.

### Dynamic Longitudinal Stability

The dynamic longitudinal stability of the airplane was characterized by a highly damped short period and a lightly damped phugoid. Figure 23 presented a time history of an elevator pulse in the landing configuration with the center of gravity at 35.2-percent MAC. The initial response indicates that the stability  $C_{m_{\alpha}}$  is near zero. The phugoid has a period of 36 seconds and damps to half amplitude in about one cycle. Figure 24 shows a time history of an elevator step with the center of gravity at 30.8-percent MAC (position used during NASA evaluation). The computed curve is for a first-order system with control effectiveness of 0.029 radian/sec<sup>2</sup> per degree of elevator and a damping time constant of 0.5. These data indicate that the stability is very low and that the initial response is approximately a first-order system. The phugoid for the center-of-gravity position at 30.8-percent MAC had a period of about 32 seconds and damped to one-half amplitude in about 2 cycles at about 58 knots; it was considered satisfactory by the evaluating pilot. The dynamic longitudinal characteristics of the airplane are influenced as was the static longitudinal stability, by the airspeed stability term  $C_{m_V}$ . This is evident in figure 23 which shows a fairly large angle-of-attack change during the phugoid. More research is required into the effect the various longitudinal stability derivatives have on handling qualities of aircraft in STOL operation.

### Stalling Characteristics

The airplane had no definitive stall in the usual sense. The stall or minimum airspeed was that airspeed at which further increases in angle of attack did not appreciably change airspeed. The lift curve is quite flat at  $C_{L_{max}}$  as shown in the discussion of the aerodynamic characteristics in the appendix. Therefore, it was difficult to determine exact angle of attack for minimum airspeed.

Figure 25 presents the stall-speed variation with engine power for take-off, landing, and wave-off configurations. At high engine power in the landing configuration, stall speeds of less than 45 knots are possible.

The only stall warning noted was some light buffeting in both landing and take-off configuration when stalls were performed at low engine power. At the higher engine power there was no natural stall warning. A stick shaker which was actuated by angle of attack was provided for stall warning. Although the pilot would desire natural stall warning, the stick shaker was considered satisfactory.

The handling qualities of the airplane near minimum airspeed were considered to be acceptable by the pilot. There was no tendency to roll-off or to pitch up or down near the stall if the sideslip angle was kept low. However, there was a tendency for the airplane to pitch up with an increase in sideslip angle at the very high angles of attack (above the angles of attack used in normal take-off rotations or landing flares). The directional stability was almost neutral near minimum airspeed, but the rudder control was adequate to control sideslip. The lateral control was also adequate near the stall, and there was sufficient longitudinal control for a rapid decrease in angle of attack for recovery.

## OPERATIONAL TECHNIQUES

### Take-Off

The take-off technique was quite easy and straightforward in that no requirement for minimum control speed had to be considered. A time history of a typical take-off is shown in figure 8. The engines can be advanced to full power and checked before the brakes are released. Nose-wheel steering which was provided by a separate control was adequate during take-off, but rudder pedal steering would have been preferable to allow the pilot to keep his left hand on the throttle. Lateral control was adequate for maintaining a wings-level attitude during the take-off roll under all crosswind conditions tested. Up elevator can be applied early in the take-off roll to obtain nose-wheel lift-off as soon as possible without an apparent drag increase. With this technique, rotation and take-off occur almost simultaneously at about 55 knots at a gross weight of 38,500 pounds. The recommended procedure is to rotate to an angle of attack between  $7^{\circ}$  and  $10^{\circ}$  and maintain this angle until the resultant climb angle has been established. Although this was considered a safe procedure, it does not produce maximum performance. In addition, angle of attack tends to overshoot initially and it is difficult to stabilize at the desired value since pitch attitude, airspeed, and angle of attack are continually changing during the rotation and lift-off. In order to obtain more consistent take-off performance a better guide is needed during rotation and lift-off. An instrument combining longitudinal acceleration with angle of attack would allow the pilot to rotate to a higher angle initially while still maintaining a safe margin from the stall.

Airspeed and angle of attack can be stabilized rapidly in the climb (65 knots and  $7^{\circ}$  angle of attack at the gross weight tested) and the airplane is easily maneuvered in this configuration. Satisfactory turn entries can be made using only lateral control, and steep turns close to the ground with bank angles up to  $45^{\circ}$  are relatively comfortable. A slight amount of bottom rudder is required to maintain steady-state turns; however, this was not particularly

objectionable to the pilot. The effect of engine failure during take-off was of relatively little concern because of the interconnected propellers; engine failure results only in a reduced rate of climb.

### Transition to Cruise

The transition to cruise is accomplished by raising the flaps in steps while maintaining angle of attack at about  $7^{\circ}$ . A time history of transition is shown in figure 26. Acceleration is smooth and rapid, and it is easy to maintain a positive climb rate throughout. The best climb speed is about 130 knots at an angle of attack of  $7^{\circ}$ . During the transition the horizontal stabilizer is repositioned to the cruise setting. It was recommended that this be done simultaneously while raising the flaps to maintain near zero stick force. This proved to be cumbersome, however, since it was to be done in a number of steps and led to some porpoising. It was easier to effect transition without retrimming the stabilizer until the flaps were fully retracted. A better solution might be to have the stabilizer programmed automatically as a function of flap position.

### Cruise

In the cruise configuration the airplane behavior resembles that of a fighter type. With spoilers only, it is quite responsive in roll and virtually no yaw is produced in turn entries or roll reversals. The longitudinal control sensitivity is considered too high for a transport airplane; however, this could probably be corrected by a variable feel system. The neutral static longitudinal stability previously discussed presented no problem under visual flight conditions; however, it would be objectionable under instrument flight conditions or during long periods of cruise.

### Transition to Landing

In order to "fit in" from a speed standpoint with the conventional aircraft traffic pattern, the transition to the landing configuration was generally performed in two steps. Flaps were lowered first to the take-off setting which allowed the speed to be reduced to about 70 knots while still allowing ample maneuverability. The downwind leg was flown at about 500 to 800 feet and well inside the faster traffic. The flaps were then fully lowered as the pilot turned onto the base leg or shortly thereafter as he commenced the final descent. Although the transition can be made in one step, as shown in figure 27, it was difficult to hold a constant altitude or glide path during such a transition, because of the trim changes associated with flap deflection and power changes.

## Approach and Landing

The approach is made by maintaining a constant angle of attack of  $3^{\circ}$  while controlling flight-path angle with power. The pilot was provided with both an angle-of-attack indicator on the instrument panel and a set of index lights which were mounted above the glare shield. The latter were more useful since they could still be seen while the pilot concentrated his vision on the landing area. Some difficulty was experienced in maintaining the correct angle of attack, as a result of the low static longitudinal stability and the trim changes associated with changes in power. This, of course, was more pronounced in turbulence and was less of a problem as more experience was obtained. The throttle-elevator interconnect seemed to alleviate this problem to some extent. There was also some difficulty in maintaining the desired flight-path angle to a given touchdown spot. There is an appreciable lag between the application of throttle and the resultant change in flight-path angle. Because of the lag there is a tendency to overcorrect which can lead to either an excessive sink rate or floating just prior to ground contact. This characteristic is evidently inherent in this class of vehicle as it has previously been reported for the C-134 and C-130 STOL aircraft (refs. 1 and 2). These comments are not meant to imply that the landing approach and touchdown are difficult to perform in this aircraft but rather to indicate areas where additional training may be required or where supplemental aids may be needed to ease the pilot's task. The Breguet technique was to adjust power to obtain the desired sink rate (800 feet per minute for maximum performance) then hold a constant angle of attack of  $3^{\circ}$  to the flare, thus ignoring to some degree the touchdown spot. With sufficient experience the pilot could probably learn to sight the airplane at the desired landing spot; however, it is felt that a visual aid (either airborne or ground based) that would indicate some desired flight-path angle would provide much more consistent accuracy. There was no opportunity to determine the minimum approach speed (or maximum approach angle of attack) for this airplane. The angle of attack used seemed to provide an adequate margin for maneuvering or gusts. From level flight at this angle of attack there appeared to be ample ability to gain altitude (well in excess of 50 feet) without the addition of power.

The flare can be initiated at about 15 to 20 feet above the runway. It was not found desirable to completely flare the aircraft but rather to rotate to the desired touchdown attitude, reducing the sink rate to 200 to 300 feet per minute at touchdown. The half-flare technique is easily accomplished but some judgment is required to estimate the initiation point in order to prevent "overflaring" and floating. If the sink rate was reduced to near zero before touchdown, it was necessary to reduce power considerably before landing. Ground effect seemed to be quite strong and there was a definite tendency to float at the speeds used. Because of this, landing from shallow approaches (less than  $4^{\circ}$ ) seemed to be more difficult to perform. During the latter portion of very flat approaches it was necessary to increase angle of attack to about  $7^{\circ}$ . When power was reduced slightly, the aircraft would then settle to the ground quite readily in a satisfactory attitude. At low angles of attack the airplane tends to land nose wheel first and bounce.

Immediately upon contacting the ground, the pilot actuates reverse pitch by rotating the throttle inboard. This can be done at any power setting and requires less than 1 second for all four propellers to reach their full reverse pitch position. As soon as it is ascertained that the propellers have reversed, full power can be applied while the anti-skid brakes are applied simultaneously to obtain maximum deceleration. The particular procedure provided for initiating reverse was considered too complicated and awkward because it was necessary to release a mechanical latch and raise the throttle grip before the throttle could be rotated. In addition, a guarded "safety" switch on top of the throttle was to be actuated when the throttle grip was rotated. Obviously any delay during each of these operations can seriously affect the landing performance. For example, a delay of 1 second results in about a 30-percent increase in ground roll. In view of this it would seem desirable in future similar STOL aircraft to have the reversing procedure simplified to reduce the number of operations required of the pilot.

### Cross-Wind Landings

Landings were performed in the test airplane with moderate cross-wind components without any difficulty. Using the crab method for cross-wind correction was somewhat objectionable because of the large angles required at low approach speeds. Rudder control power was adequate, however, to decrab before touchdown. Another technique used was essentially the wing-down method, but it was modified to some extent in that sideslip rather than bank angle was used as the primary control parameter. Figure 28 presents the sideslip and bank angle required as a function of cross-wind component. These data, which were obtained from steady-state sideslips, show that the bank angle required is quite small in comparison to the corresponding sideslip angle. Consequently it was quite difficult for the pilot to judge the correct amount of bank angle for counteracting the cross wind. It was much easier to establish the sideslip required to maintain the desired track on the final approach and then maintain heading with bank attitude. If the pilot knows the cross-wind component and has a sideslip indicator he can trim the aircraft into the required sideslip prior to reaching the final approach. A simple rule of thumb would be  $1^\circ$  of sideslip for each knot of cross wind. This technique makes cross-wind landings very similar to normal STOL landings during the final approach.

### Wave-Off

In order to establish a satisfactory rate of climb in the event of a three-engine go-around, the wave-off procedure called for reducing the flap deflection to 75/50 while simultaneously adding maximum power. This was accomplished with a thumb operated, momentary type switch on the throttle grip which could control the flaps between 98/65 and 75/50. This was considered an acceptable procedure since there were no noticeable lift or trim changes associated with the flap angle change. It would be desirable, however, to initiate flap retraction during the wave-off without requiring the pilot to perform an additional operation which

might be overlooked in an emergency. The addition of full power would normally result in an undesirably large nose-down pitching moment. To compensate for this moment, a throttle-elevator interconnect was incorporated which repositioned the elevator feel bungee to reduce the trim force. Time histories of wave-offs performed with hands-off-the-stick both with and without the device are shown in figure 22. The immediate favorable pitch attitude response provided by the interconnect was considered satisfactory.

#### CONCLUDING REMARKS

A flight investigation of a typical STOL transport aircraft was undertaken, utilizing the Breguet 941 airplane. The study has shown that the airplane has acceptable performance, handling qualities, and operational characteristics for the STOL mission. The evaluating pilot found the airplane comfortable to fly at the low airspeeds required for STOL operation. Many of the satisfactory characteristics can be attributed either directly or indirectly to the cross shafting of the propellers. The safety aspect of interconnecting the propellers is obvious in case of engine failure and adds much to the pilot's sense of well being when flying at low airspeeds and high power. Lateral control power and adverse yaw characteristics are improved to a satisfactory level by the use of differential propeller pitch. Finally, opposite rotating propellers gave aerodynamic symmetry and no lateral or directional moment changes with changes in airspeed or engine power.

The pilot considered both longitudinal and lateral-directional stability too low for a completely satisfactory rating. Low stability, particularly inherent in an airplane with high moments of inertia operating at low airspeeds, results in low restoring moments and long periods which complicate the pilot's control task. More research is required to determine ways to cope with the problem and to adequately define stability and control requirements of STOL airplanes.

Ames Research Center  
National Aeronautics and Space Administration  
Moffett Field, Calif., Nov. 18, 1963

## APPENDIX

### LIFT AND DRAG CHARACTERISTICS

The lift and drag characteristics of the airplane at various values of thrust coefficient in the take-off, landing, and wave-off configurations are shown in figure 29. Lift and drag curves at constant engine power are also shown. These data were cross plotted from flight test data. It should be pointed out that the angle of attack,  $\alpha_u$ , used in these data is uncorrected vane angles obtained from an angle-of-attack vane mounted on a nose boom about 6 feet in front of the airplane. The uncorrected angle-of-attack reading was used because an accurate flight calibration of the vane was not made. An approximate calibration of the vane as derived from Breguet wind-tunnel data is shown in figure 30. The maximum lift capabilities of the Breguet 941 are summarized in figure 31 which presents the variation of  $C_{L_{max}}$  with thrust coefficient for various flap deflections. The values of  $C_{L_{max}}$  at high thrust coefficients were taken where the lift-curve slope approached zero since there was not a usual lift-curve peak to define  $C_{L_{max}}$ . The values of  $C_{L_{max}}$  were 5 and 6.7 with maximum engine power in the take-off and landing configurations, respectively, at about 5000 feet altitude and at a gross weight of 38,500.

Figure 32 shows a computed drag polar for the airplane in the cruise configuration with measured flight test data points for comparison. The airplane in the cruise configuration had a  $C_{L_{max}}$  of about 1.6 which occurred at an indicated angle of attack of  $23^\circ$ .

## REFERENCES

1. Innis, Robert C., and Quigley, Hervey C.: A Flight Examination of Operating Problems of V/STOL Aircraft in STOL Landing and Approach. NASA TN D-862, 1961.
2. Quigley, Hervey C., and Innis, Robert C.: Handling Qualities and Operational Problems of a Large Four-Propeller STOL Transport Airplane. NASA TN D-1647, 1963.
3. Quigley, Hervey C., and Lawson, Herbert F.: Simulator Study of the Lateral-Directional Handling Qualities of a Large Four-Propeller STOL Transport Airplane. NASA TN D-1773, 1963.
4. Turner, Howard L., and Drinkwater, Fred J., III.: Some Flight Characteristics of a Deflected Slipstream V/STOL Aircraft. NASA TN D-1891, 1963.
5. Lecomte, P. E.: Recent French Experience in the Field of V/STOL Aircraft. Paper No. 670B presented at the National Aero-Nautical Meeting of the Society of Automotive Engineers and American Society of Naval Engineers, April 8-11, 1963 (A63-14438).
6. Ziegler, Henri: The Fourteenth Louis Blériot Lecture: The Development of Short Range Air Transport Through the Use of V/STOL Aircraft. Jour. Roy. Aero. Soc., vol. 65, no. 605, May 1961, pp. 305-320.
7. Weiberg, James A., and Holzhauser, Curt A.: STOL Characteristics of a Propeller-Driven, Aspect-Ratio-10, Straight-Wing Airplane With Boundary-Layer Control Flaps, as Estimated From Large-Scale Wind-Tunnel Tests. NASA TN D-1032, 1961.
8. Cooper, George E.: Understanding and Interpreting Pilot Opinion. Aero. Eng. Rev., vol. 16, no. 3, March 1957, pp. 47-51, 56.
9. Weiberg, James A., and Page, V. Robert: Large-Scale Wind-Tunnel Tests of an Airplane Model With an Unswept, Aspect-Ratio-10 Wing, Four Propellers, and Blowing Flaps. NASA TN D-25, 1959.

TABLE I. - GEOMETRIC DATA

Wing	
Area, sq ft . . . . .	889
Span, ft . . . . .	76.1
Mean aerodynamic chord (reference), ft . . . . .	12.15
Incidence root, from fuselage reference line, deg . . . . .	3
Twist, deg . . . . .	0
Dihedral, deg . . . . .	4
Airfoil section with cambered leading edge from internal nacelle to wing tip . . . . .	
	63A416
Aspect ratio . . . . .	6.52
Taper ratio . . . . .	0.507
Flap deflection (maximum), deg . . . . .	Internal 98; external 65
Flap chord (percent wing chord) . . . . .	38.5
Spoiler spanwise location . . . . .	From 56 to 97 percent of span
Spoiler deflection, deg . . . . .	45
Spoiler chord, percent chord . . . . .	7
Horizontal tail	
Total area, sq ft . . . . .	320
Span, ft . . . . .	32.8
Mean aerodynamic chord, ft . . . . .	9.92
Airfoil section . . . . .	63A212 inverted with cambered leading edge
Elevator area, sq ft . . . . .	119
Elevator deflection, deg	
Maximum trailing edge up . . . . .	-35
Maximum trailing edge down . . . . .	+25
Stabilizer deflection, deg . . . . .	+1 to +9 to fuselage ref. (leading edge up)
Vertical tail	
Total area, sq ft . . . . .	219
Span, ft . . . . .	17.9
Mean aerodynamic chord, ft . . . . .	13.1
Airfoil section (modified) . . . . .	63A013
Rudder area, sq ft . . . . .	82.6
Rudder deflection, deg	
First rudder . . . . .	±20
Second rudder . . . . .	±40
Moment of inertia (approximate for 38,500 lb gross weight)	
I <sub>xx</sub> , slug-ft <sup>2</sup> . . . . .	225,000
I <sub>yy</sub> , slug-ft <sup>2</sup> . . . . .	140,000
I <sub>zz</sub> , slug-ft <sup>2</sup> . . . . .	400,000

TABLE II.- PILOT OPINION RATING SYSTEM FOR UNIVERSAL USE

	Adjective rating	Numerical rating	Description	Primary mission accomplished	Can be landed
Normal operation	Satisfactory	1	Excellent, includes optimum	Yes	Yes
		2	Good, pleasant to fly	Yes	Yes
		3	Satisfactory, but with some mildly unpleasant characteristics	Yes	Yes
Emergency operation	Unsatisfactory	4	Acceptable, but with unpleasant characteristics	Yes	Yes
		5	Unacceptable for normal operation	Doubtful	Yes
		6	Acceptable for emergency condition only <sup>1</sup>	Doubtful	Yes
No operation	Unacceptable	7	Unacceptable even for emergency condition <sup>1</sup>	No	Doubtful
		8	Unacceptable - dangerous	No	No
		9	Unacceptable - uncontrollable	No	No

<sup>1</sup>Failure of a stability augments

TABLE III.- LATERAL CONTROL CHARACTERISTICS FOR VARIOUS CONFIGURATIONS

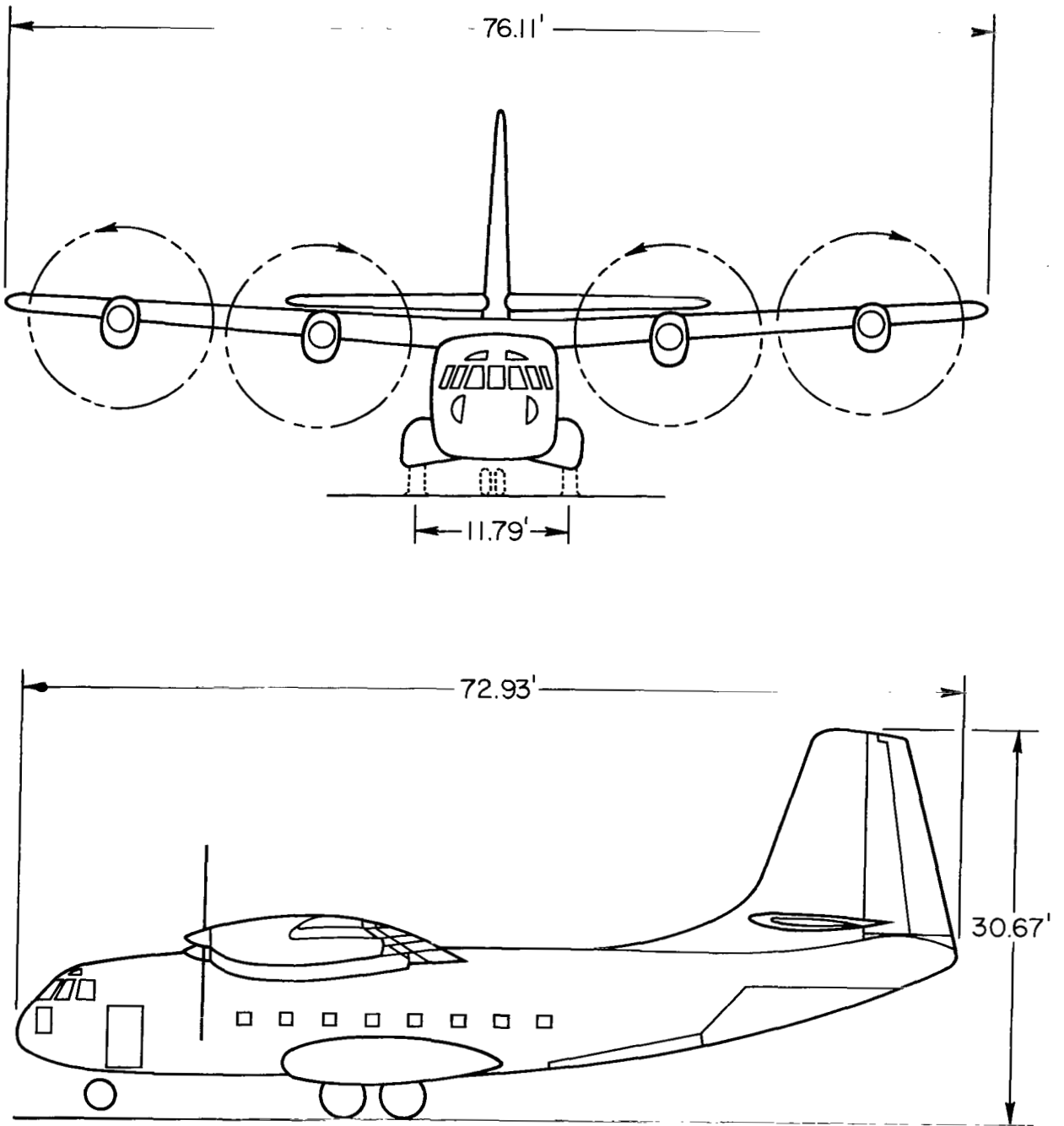
Configuration	Ailerons	Spoilers	Differential propeller pitch	Control power, radians/sec <sup>2</sup>	Sensitivity, radians/sec <sup>2</sup> /in.	Pilot's rating
Landing	On	On	On	0.42	0.14	3
	Off	On	On	.40	.12	3-1/2
	On	On	Off	.32	.09	5
	On	Off	On	.17	.03	7-1/2
Take-off	On	On	On	.65	.19	2-1/2
	Off	On	On	.44	.13	3
Cruise	On	On	On		.21	4
	Off	On	Off		.125	2



A-31451

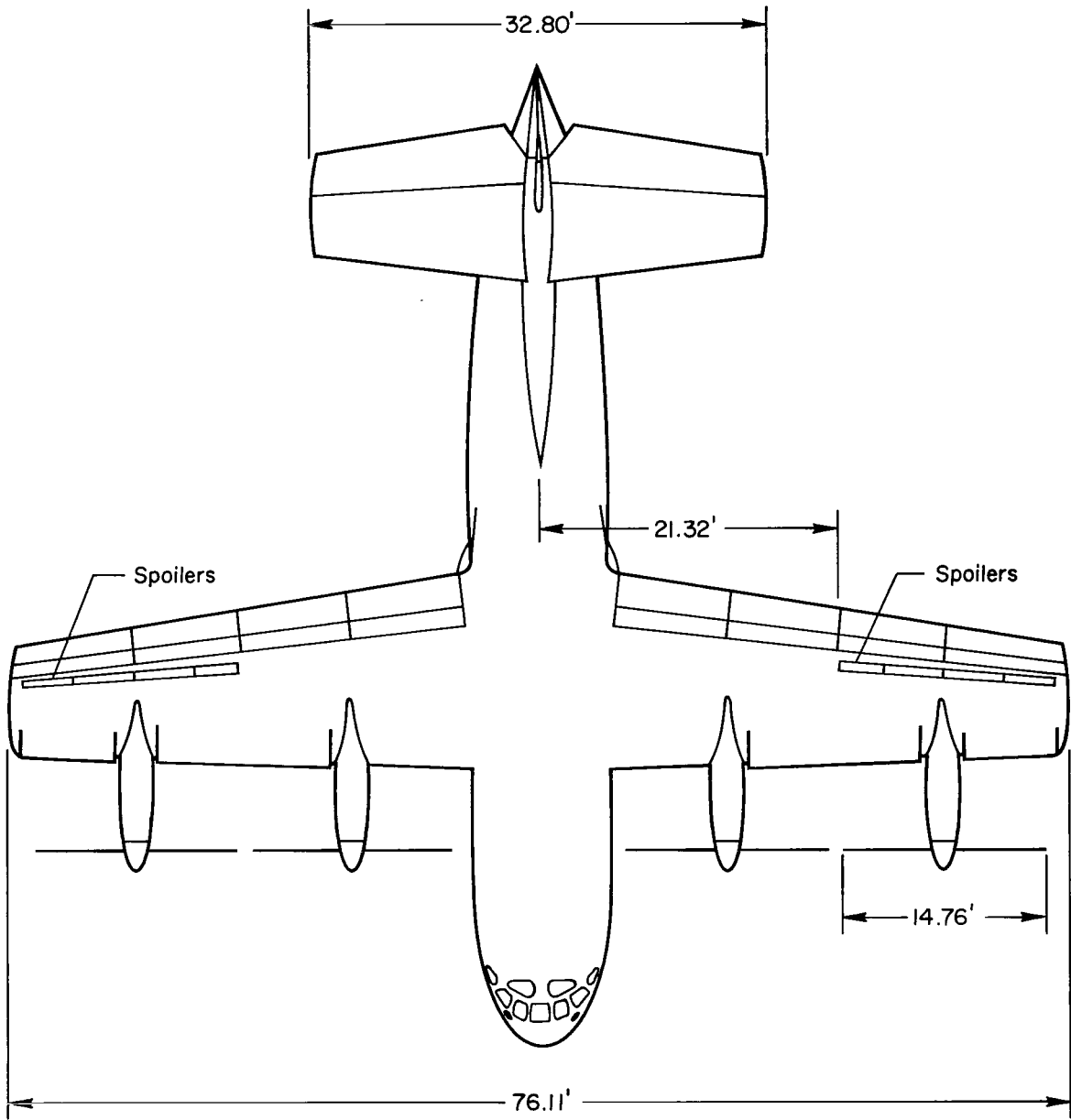
5

Figure 1.- Photograph of test airplane in landing configuration,  $\delta_F = 98/65$ .



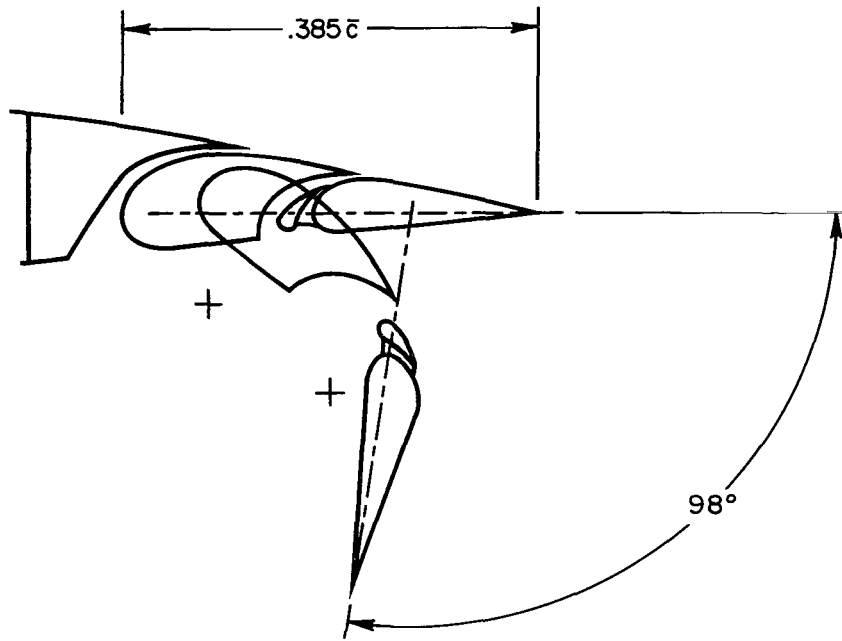
(a) Front and side view.

Figure 2.- Sketch of test airplane.

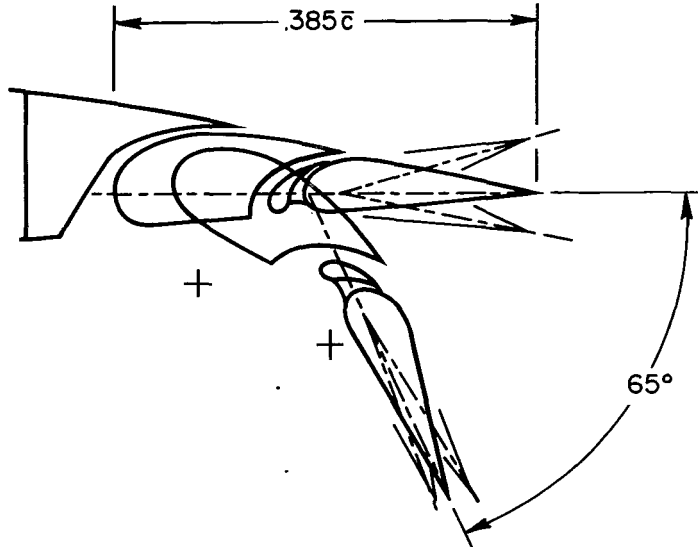


(b) Top view.

Figure 2.- Concluded.

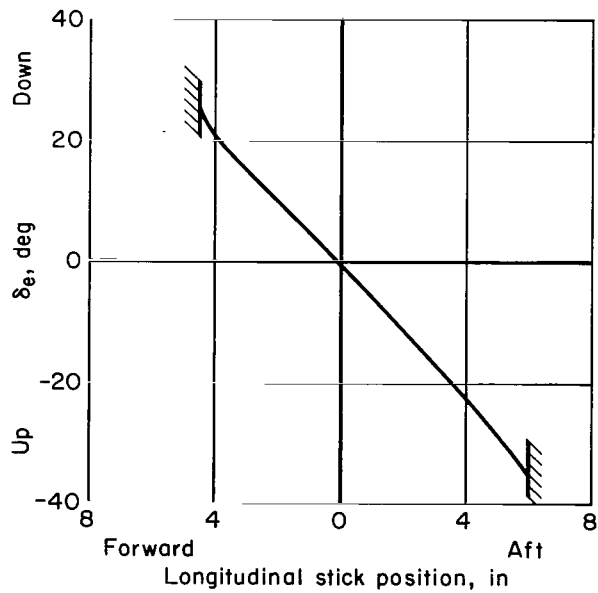
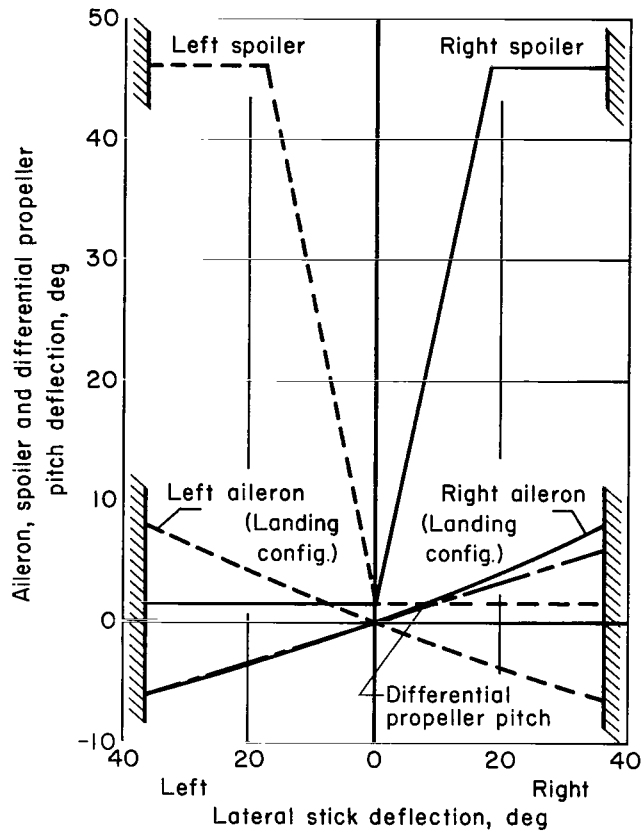


(a) Inboard flap.



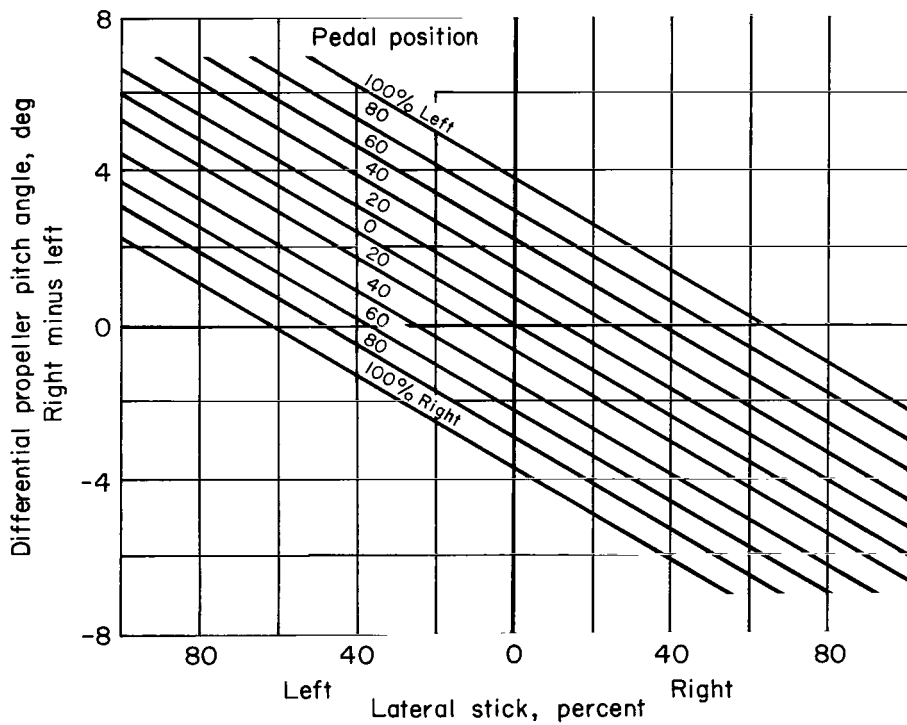
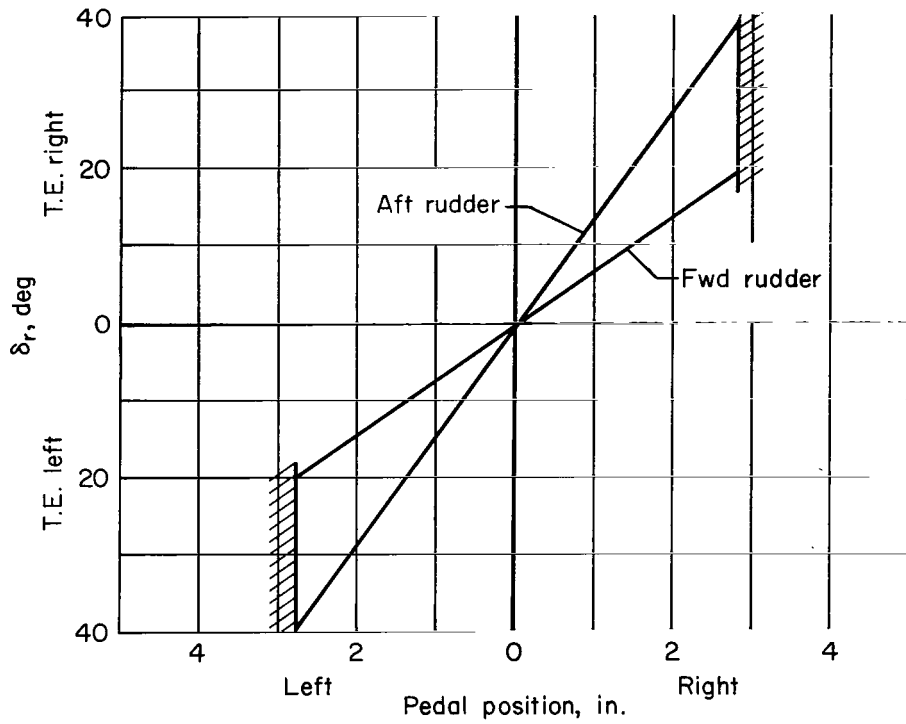
(b) Outboard-flap aileron.

Figure 3.- Cross section of the trailing-edge flap in a landing configuration;  
 $\delta_f = 98/65$ .



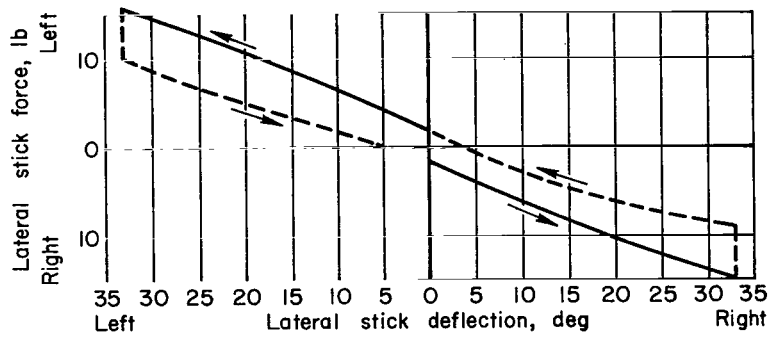
(a) Lateral and longitudinal control.

Figure 4.- Control displacements variation with control input.

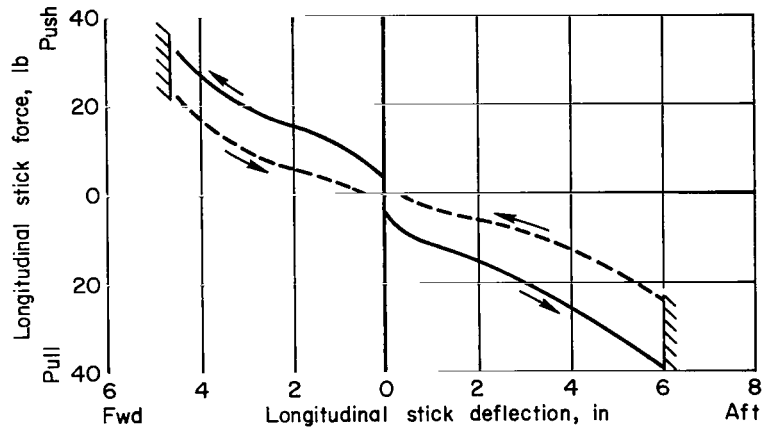


(b) Rudder and differential propeller pitch angle.

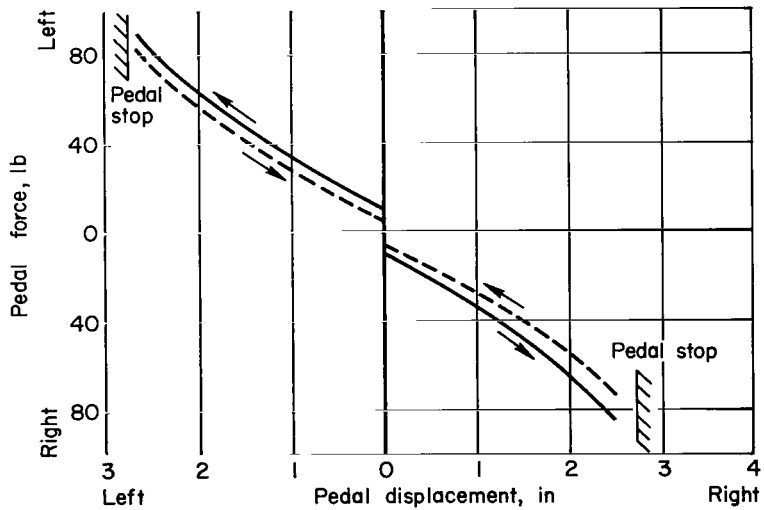
Figure 4.- Concluded.



(a) Lateral.



(b) Elevator.



(c) Pedal displacement.

Figure 5.- Force characteristics of flight control system.

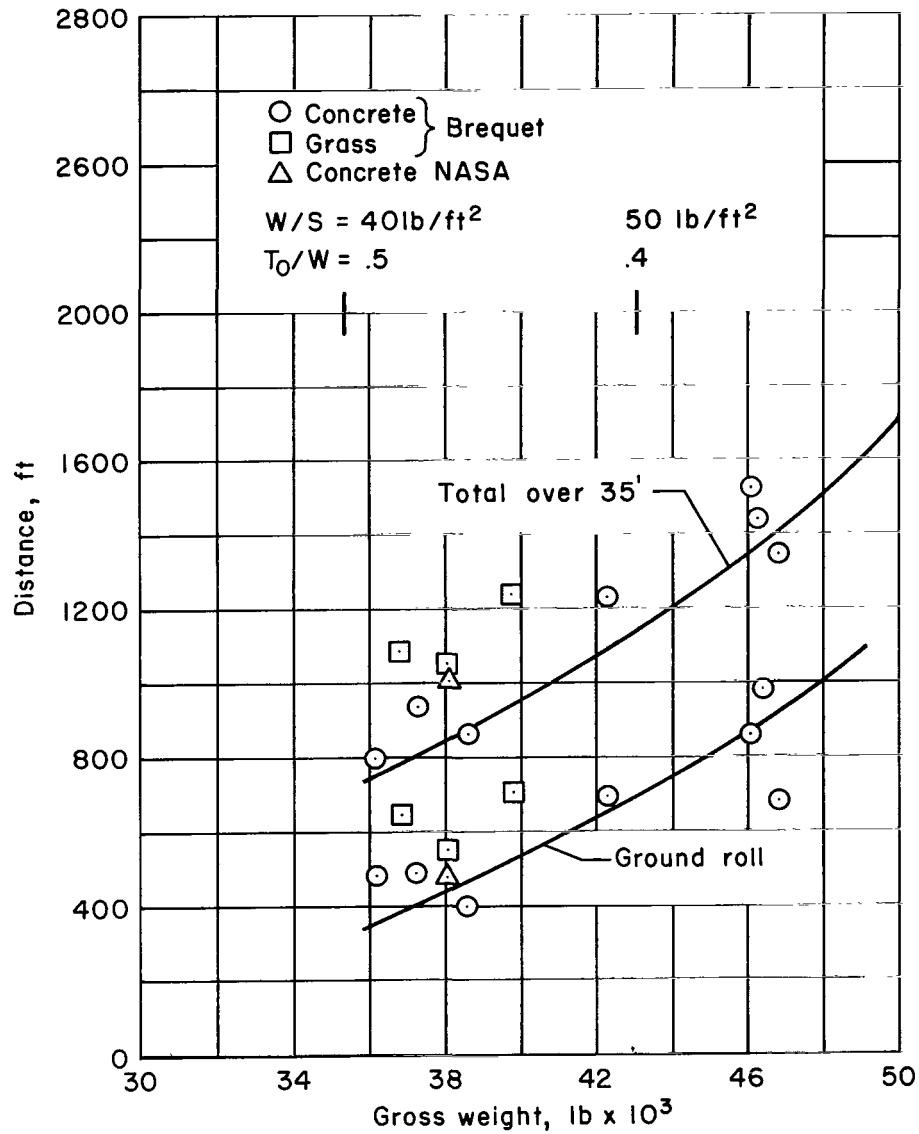


Figure 6.- Take-off distance variation with gross weight; average shaft horsepower per engine = 1,100,  $\delta_F = 45/30$  corrected for wind.

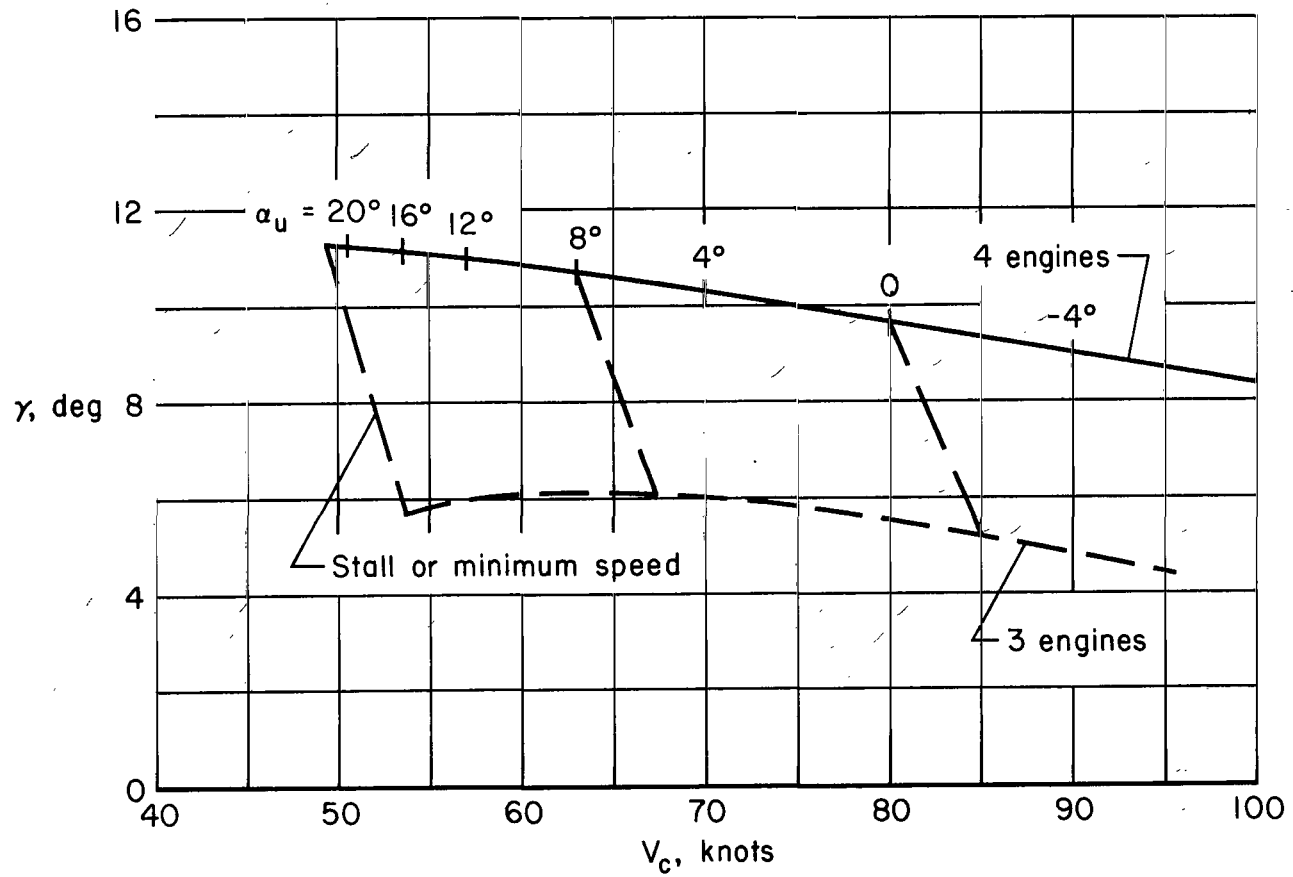


Figure 7.- Operational take-off envelope;  $W = 38,500$  lb,  $\delta_F = 45/30$ , 1,100 shaft horsepower per engine.

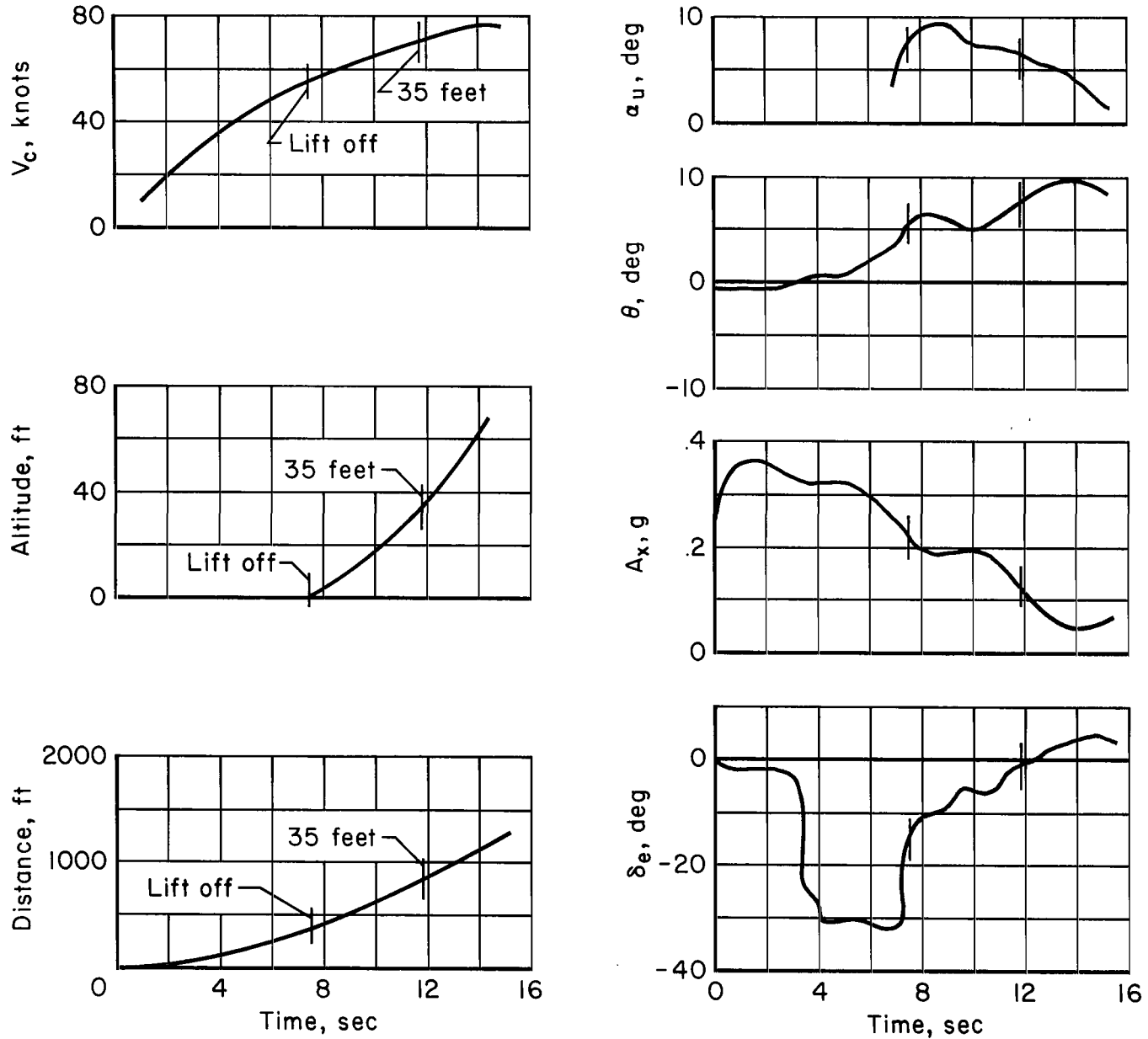


Figure 8.- Take-off time history;  $W = 38,600$  lb,  $\delta_f = 45/30$ ,  $i_t = 0^\circ$ , 1,080 shaft horsepower per engine.

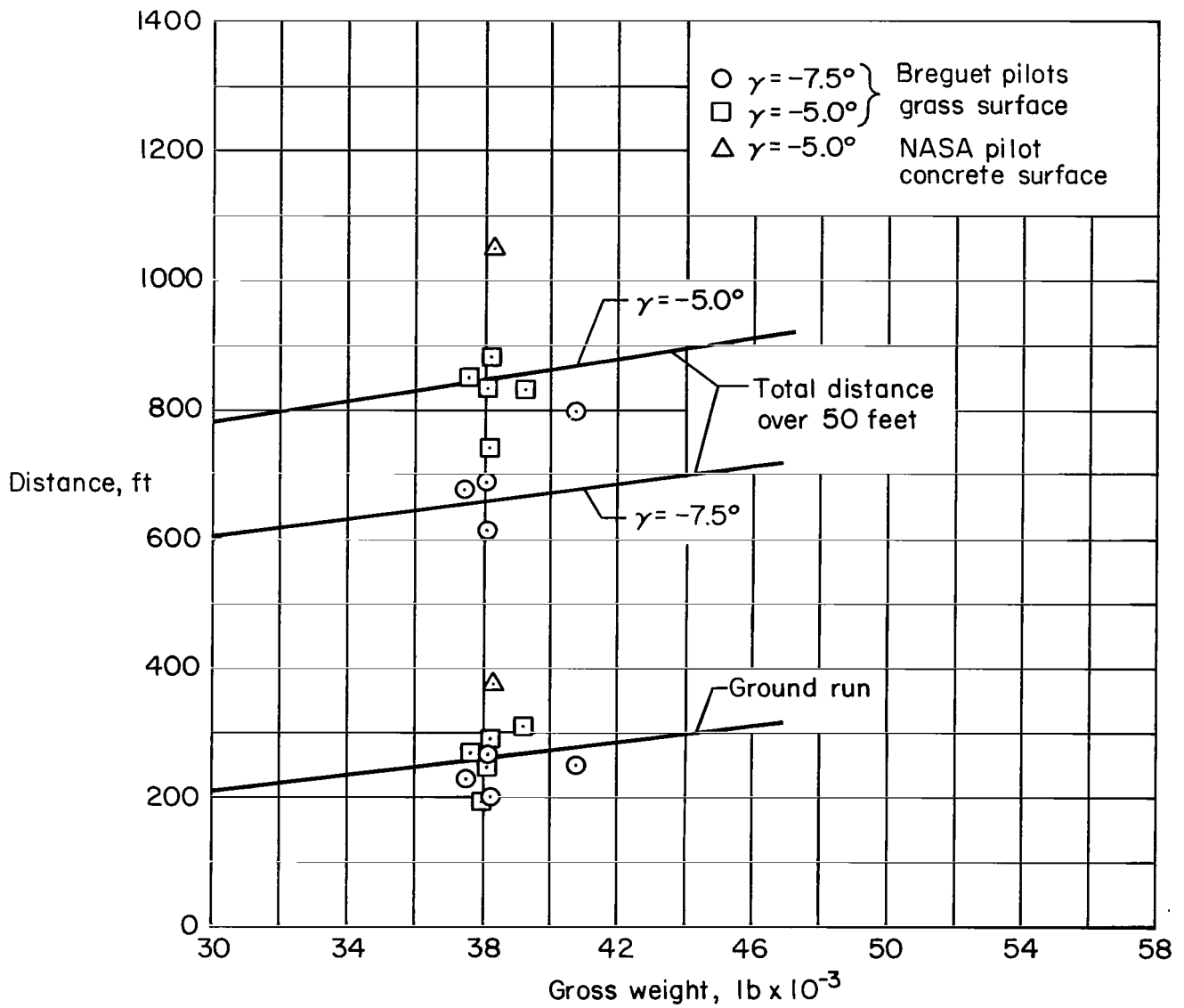


Figure 9.- Landing distance variation with gross weight;  $\delta_F = 98/65$  corrected for wind, sea level.

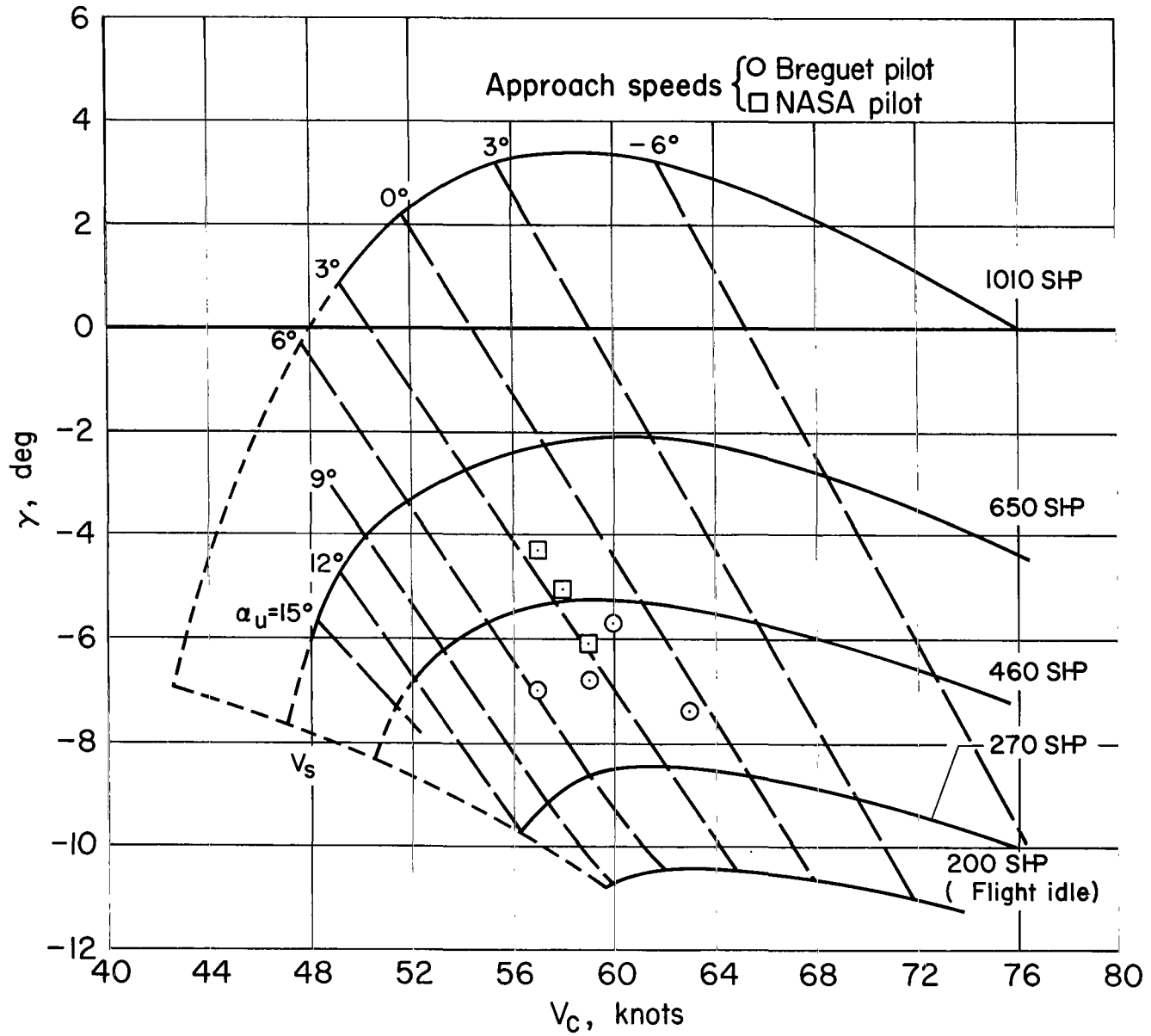


Figure 10.- Landing operational envelope;  $W = 38,500$  lb,  $\delta_f = 98/65$ .

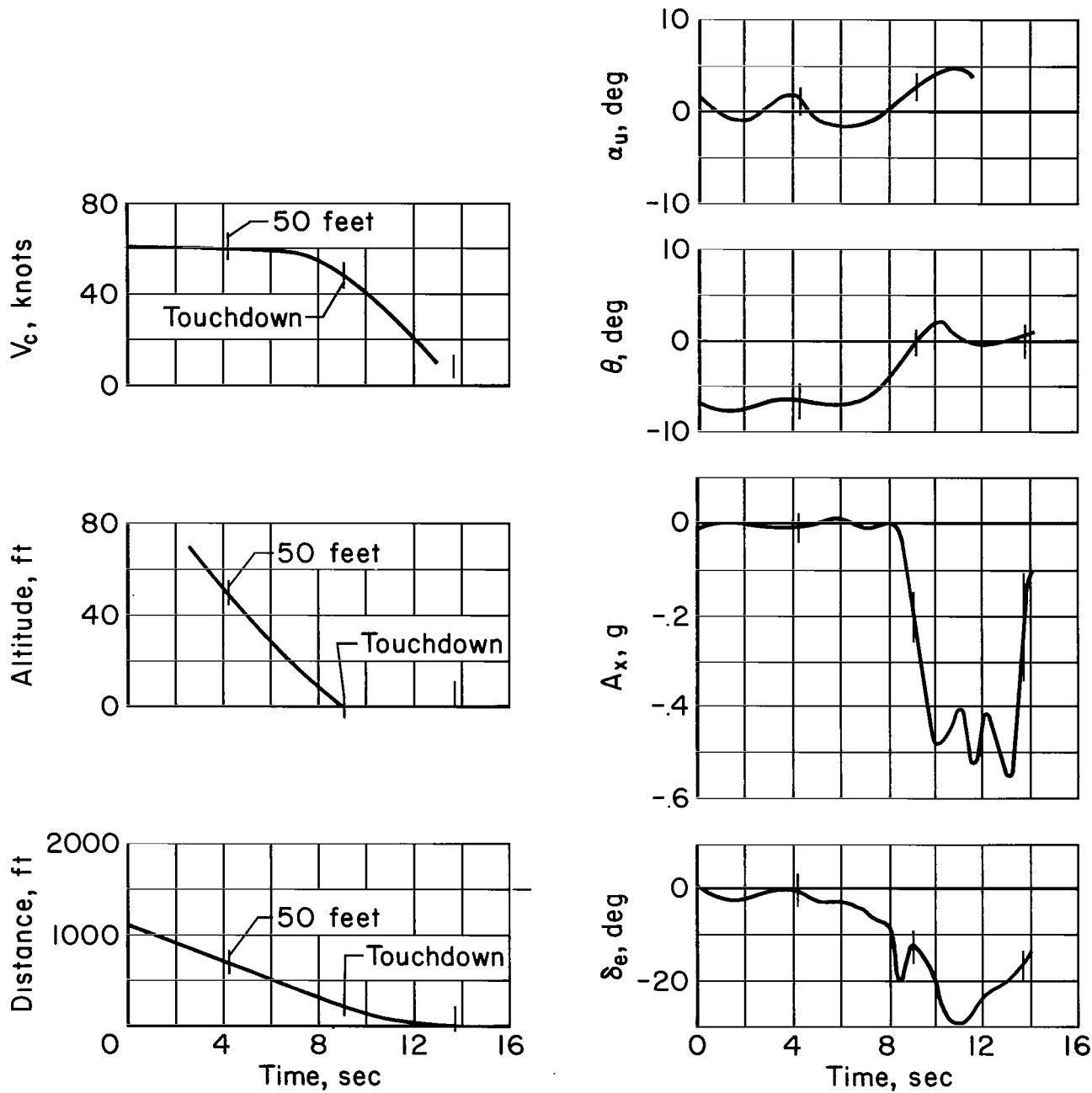


Figure 11.- Landing time history;  $W = 37,600$  lb,  $\delta_F = 98/65$ ,  $i_t = 9.0^\circ$ ,  
 370 shaft horsepower per engine.

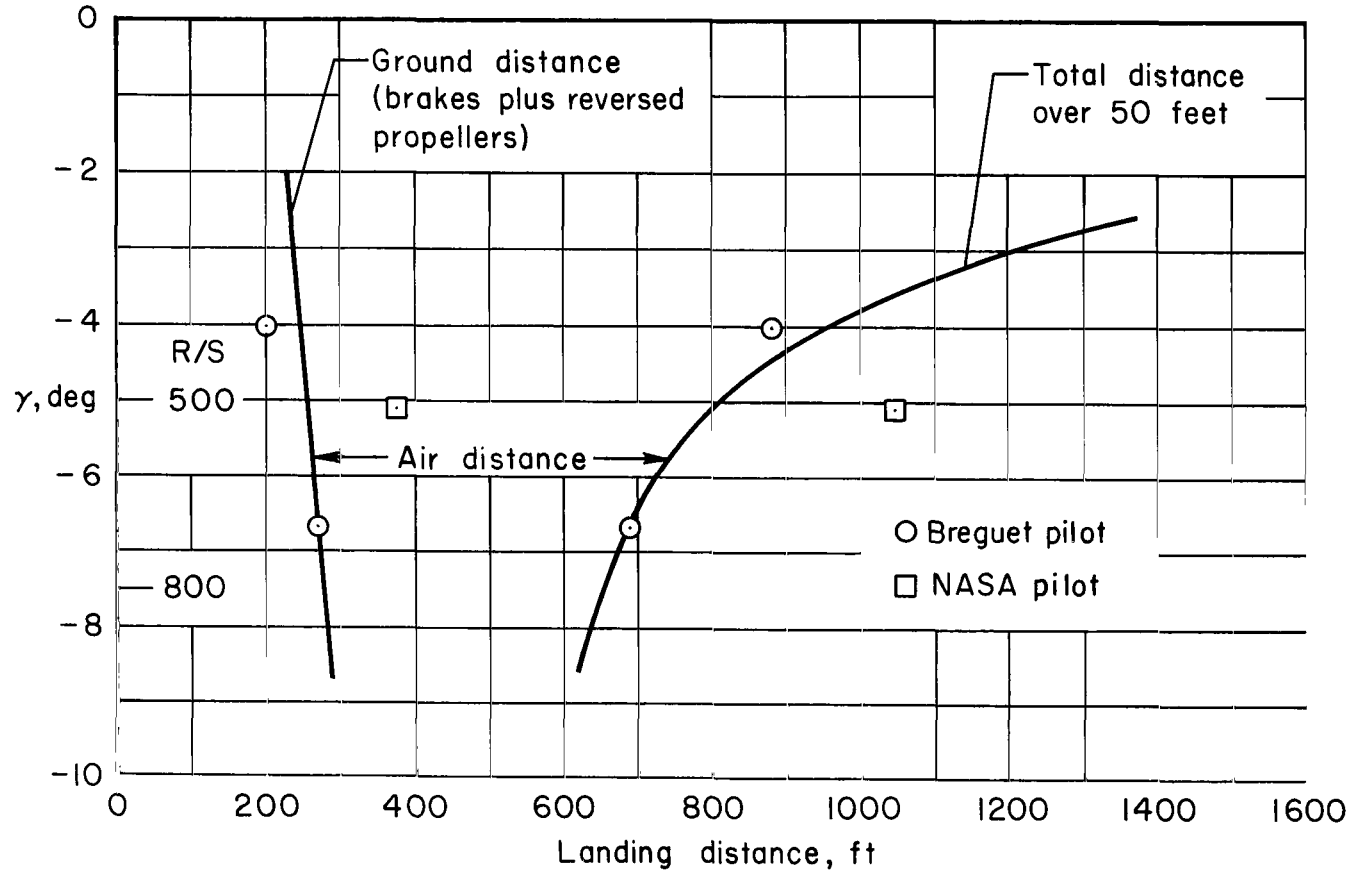


Figure 12.- Variation of landing distance with flight path angle;  $\delta_f = 98/65$ ,  $\alpha_u = 3^\circ$ ,  $W = 38,500$  lb.

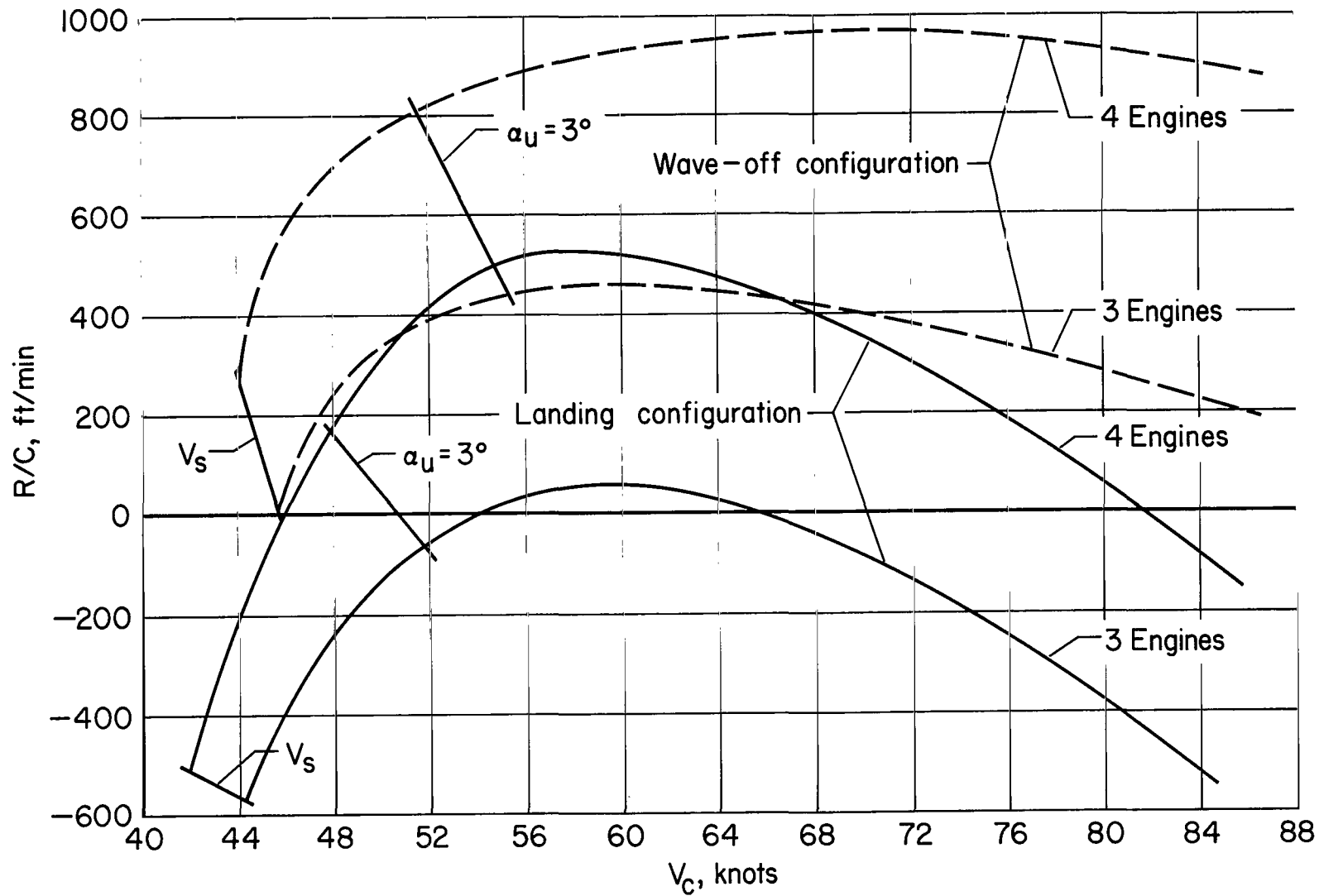


Figure 13.- Comparison of wave-off with landing operational envelope at wave-off power (1,100 shaft horsepower per engine);  $W = 38,500$  lb.

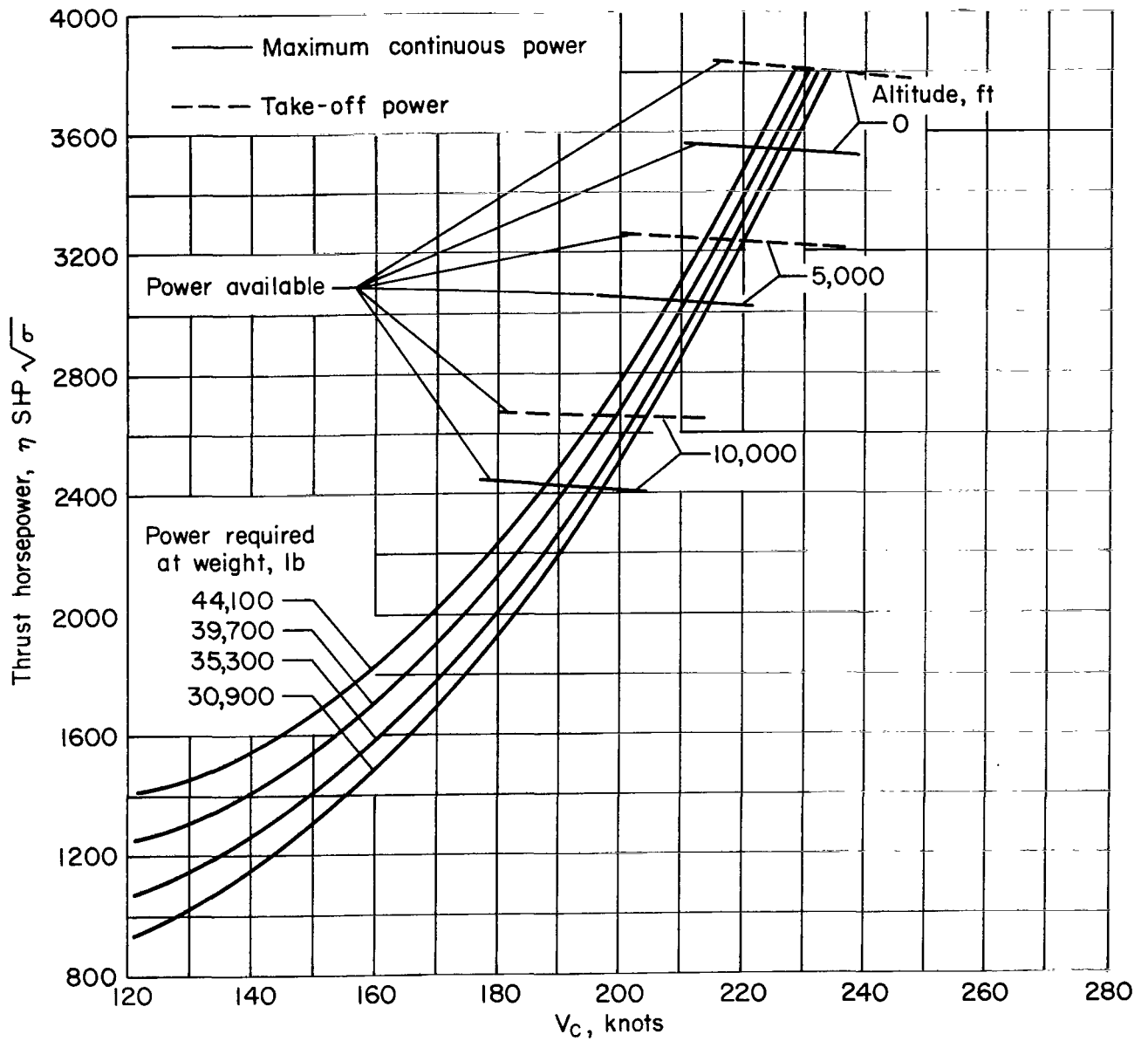
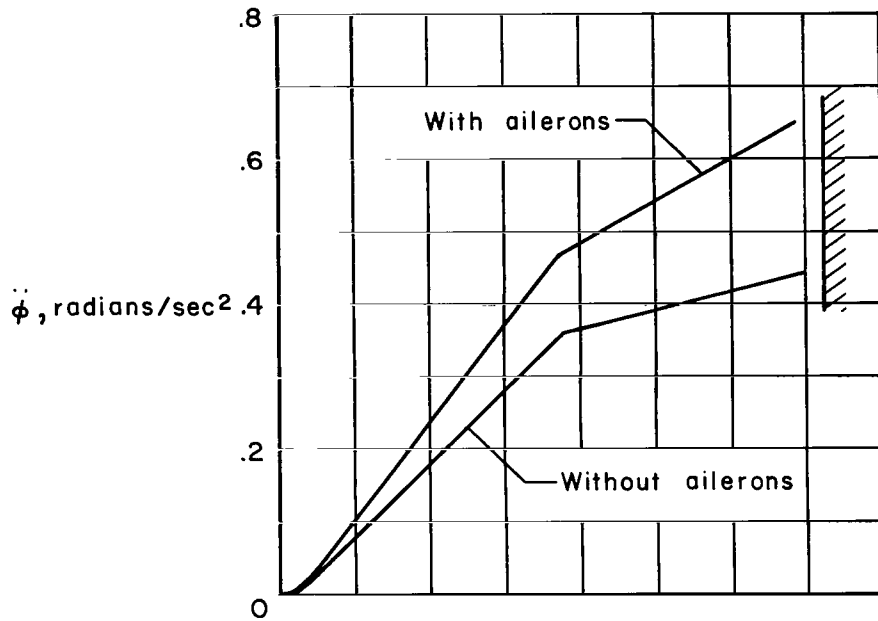
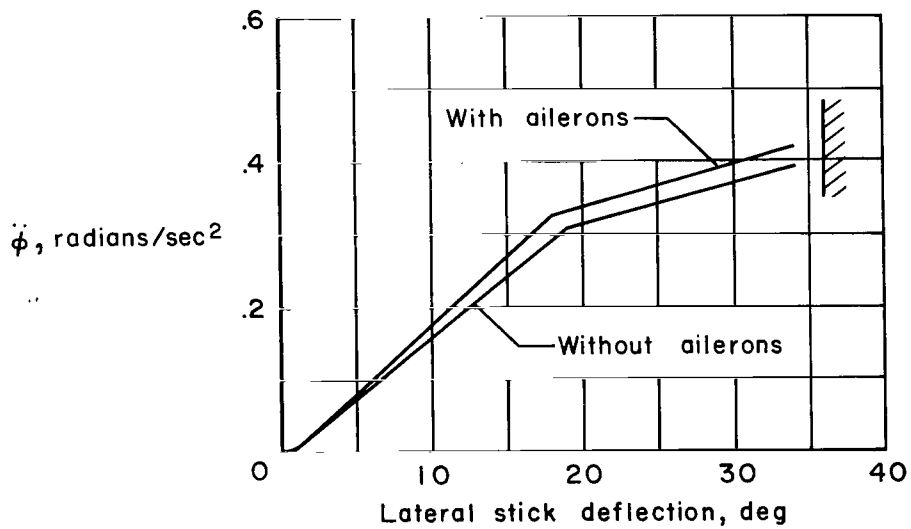


Figure 14.- Variation of power required and power available with airspeed, altitude, and gross weight in cruise.



(a) Take-off configuration;  $\delta_f = 45/30$ ,  $V_c \approx 70$  knots.



(b) Landing configuration;  $\delta_f = 98/65$ ,  $V_c \approx 60$  knots.

Figure 15.- Variation of initial angular acceleration with lateral stick deflection;  $\alpha_u \approx 3^\circ$ .

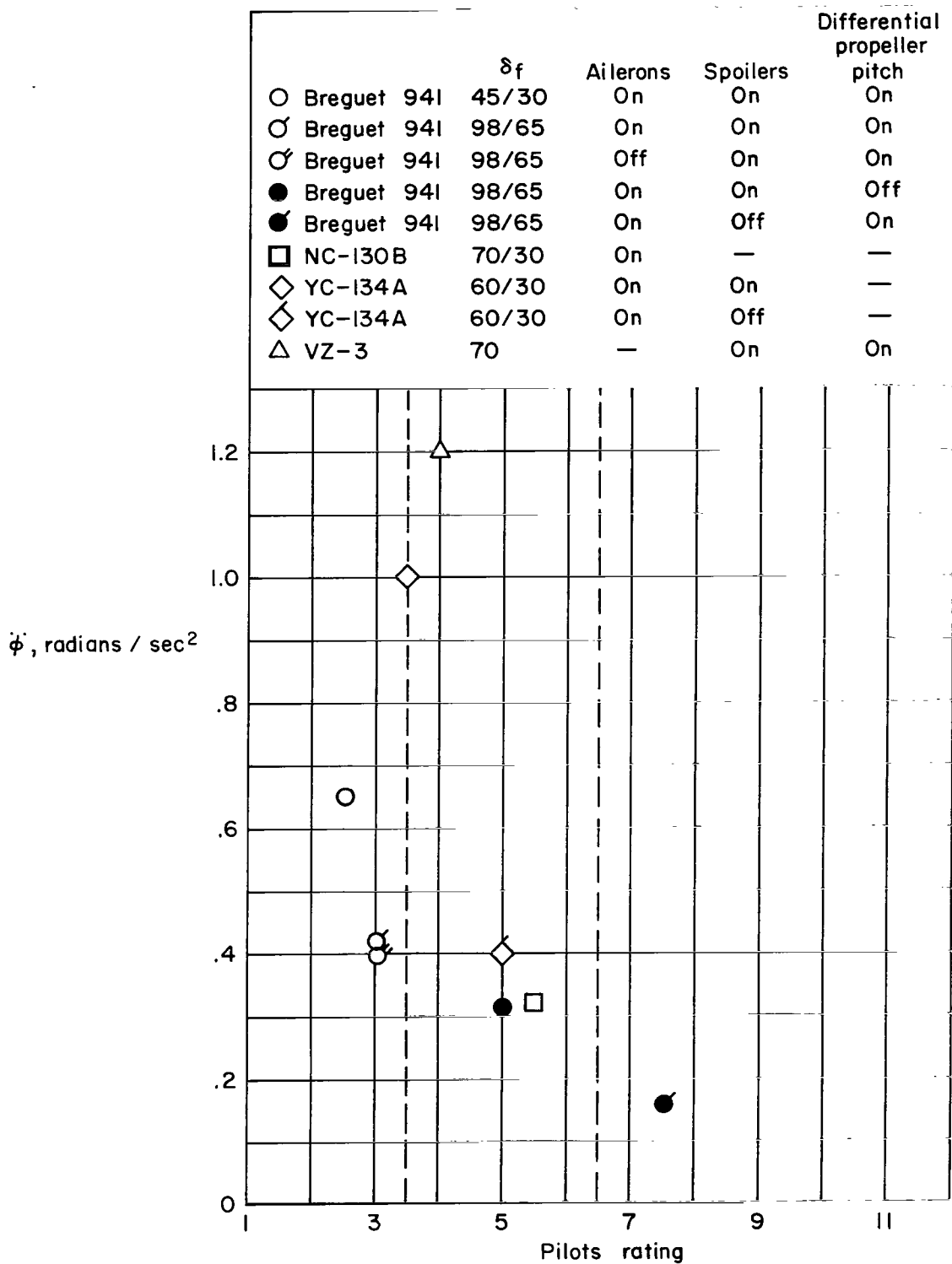


Figure 16.- Pilot's rating of lateral control power for several STOL aircraft operating in the 40- to 70-knot airspeed range.

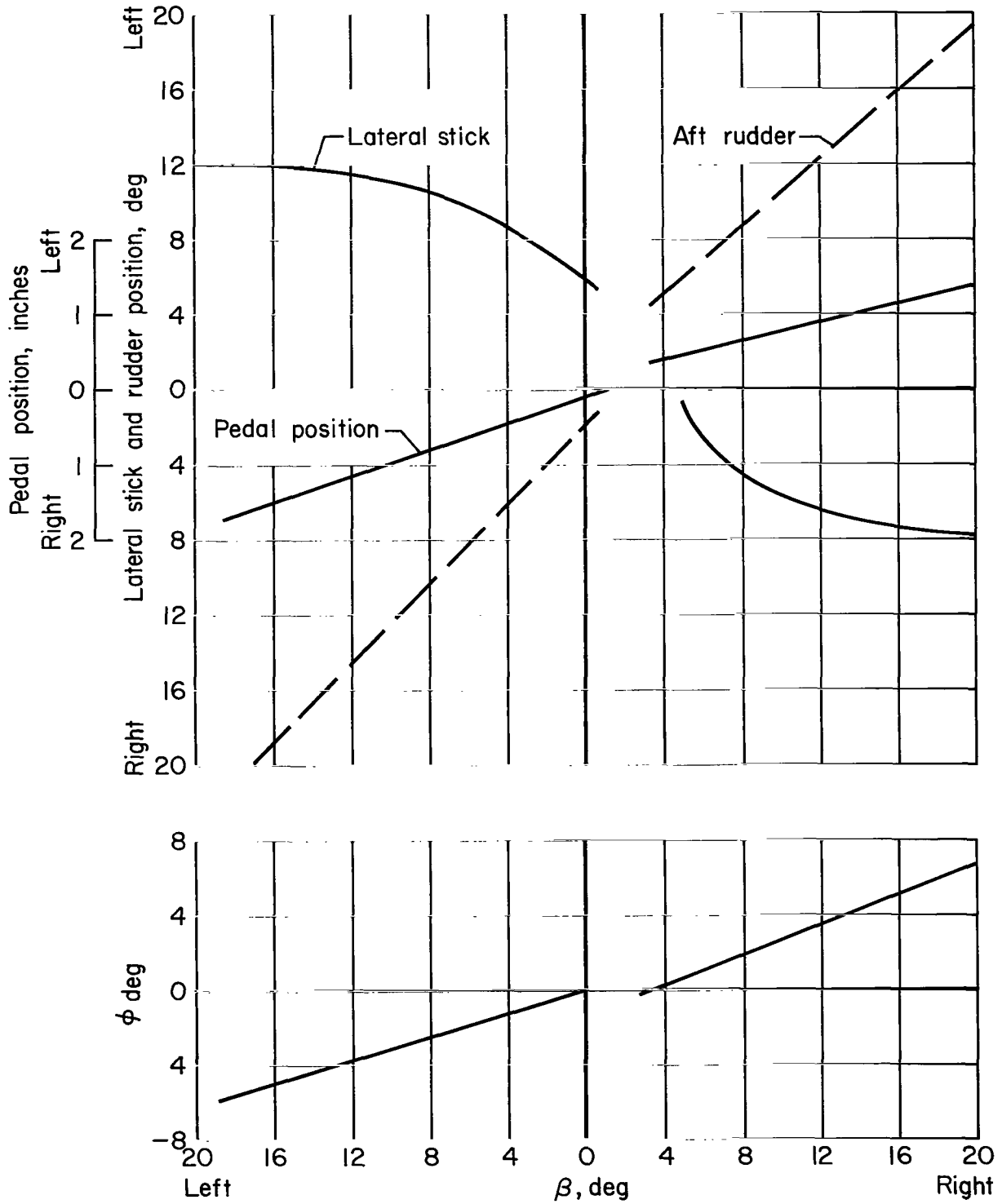


Figure 17.- Steady-state sideslips in landing configuration;  $\delta_f = 98/65$ ,  
 $\alpha_u = -0.5$ ,  $V_c = 62$  knots.

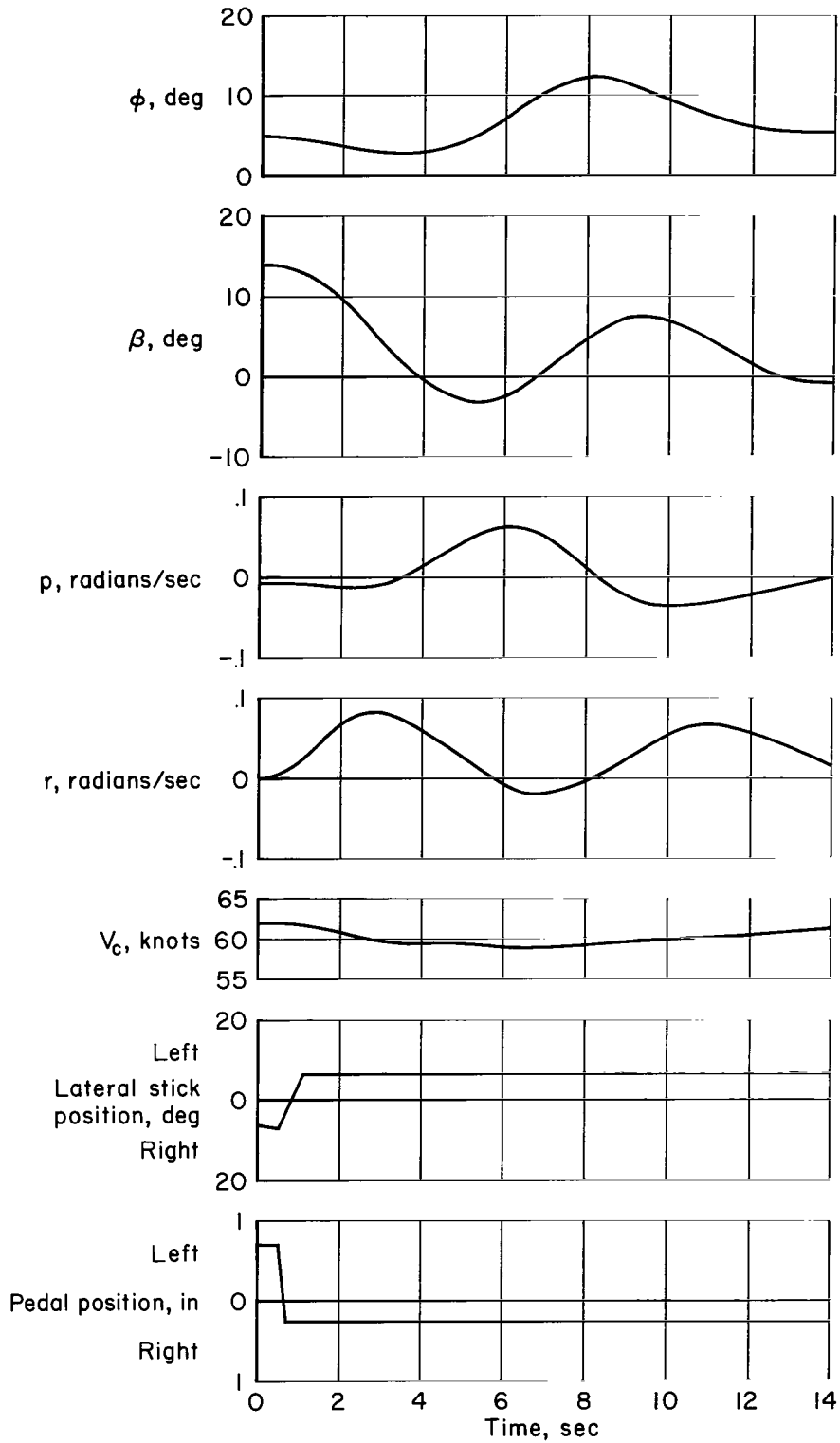


Figure 18.- Time history of lateral-directional oscillation following release from steady-state sideslip; landing configuration,  $\delta_f = 98/65$ .

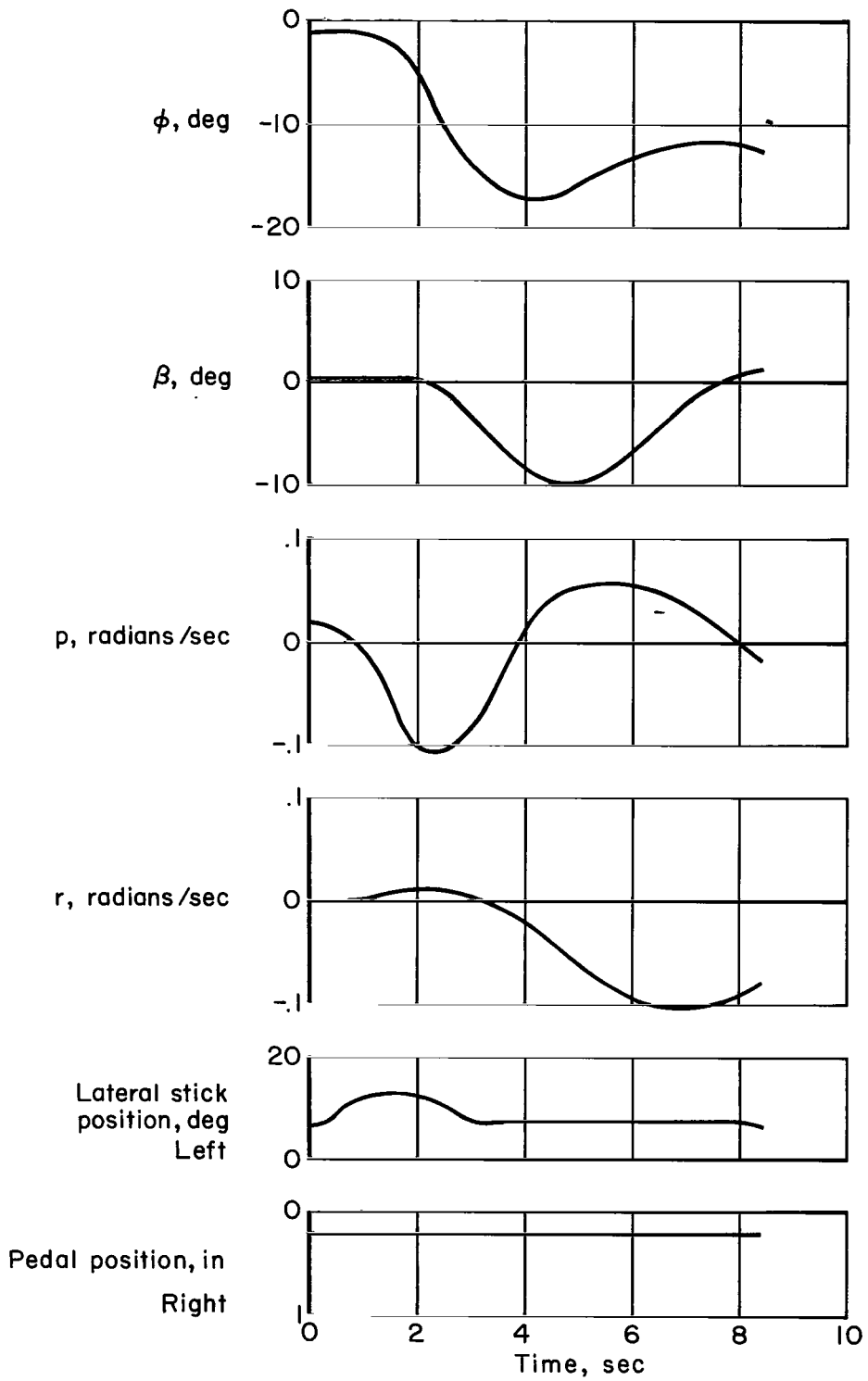
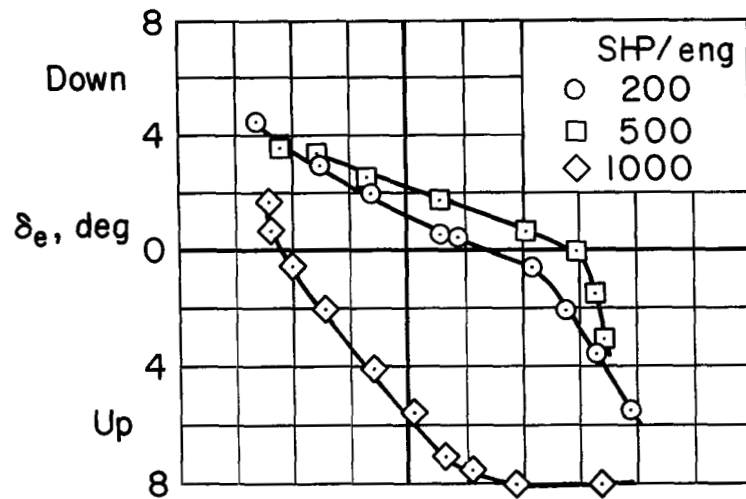
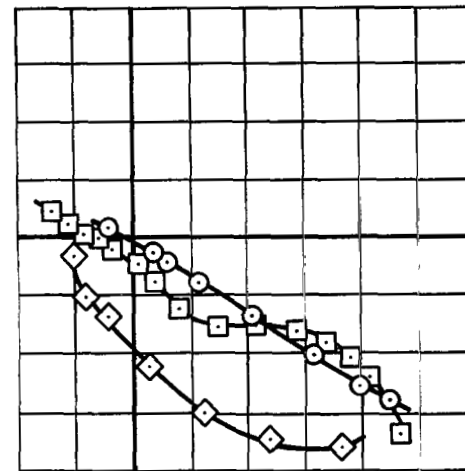


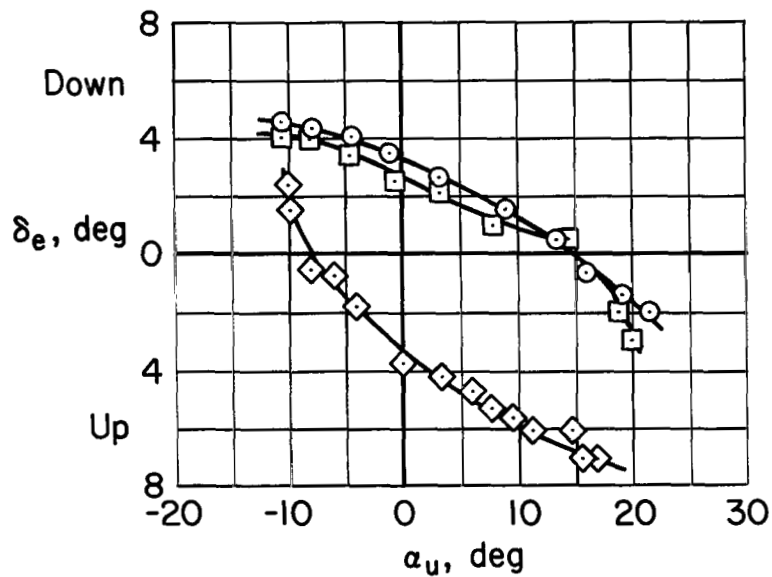
Figure 19.- Time history of lateral-directional oscillation following pulse lateral stick input; landing configuration,  $\delta_F = 98/65$ ,  $V_c = 60$  knots.



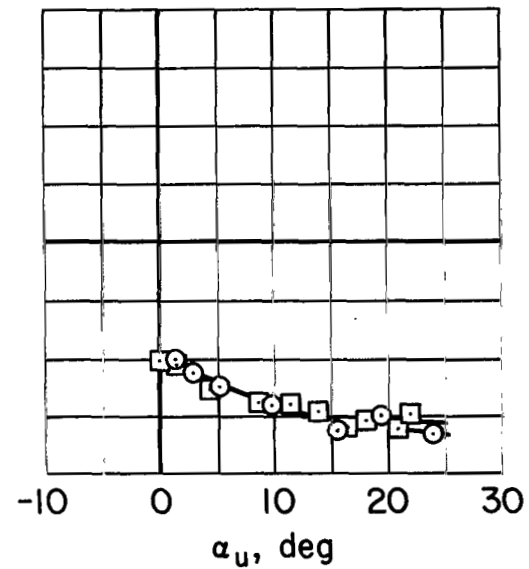
$\delta_f = 98/65$ ;  $W \approx 37,000$  lb;  $i_t = 7.6^\circ$



$\delta_f = 45/30$ ;  $W \approx 36,000$  lb;  $i_t = 5.6^\circ$

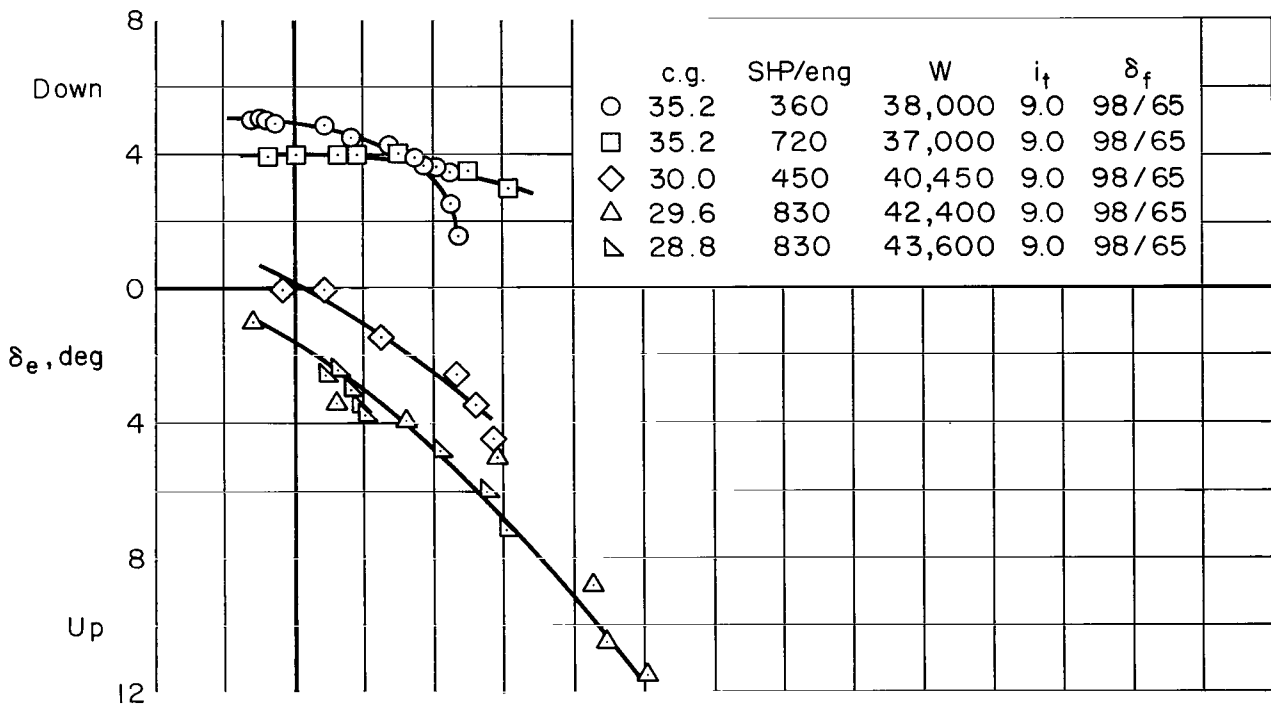


$\delta_f = 75/50$ ;  $W \approx 38,000$  lb;  $i_t = 6.0^\circ$

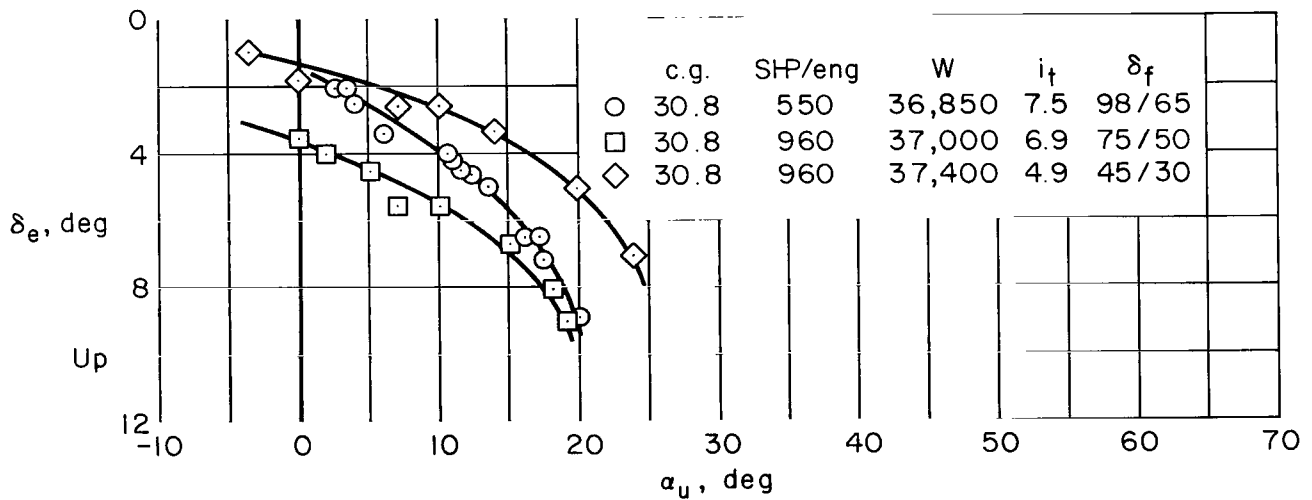


$\delta_f = 25/17$ ;  $W \approx 36,000$  lb;  $i_t = 5.9^\circ$

Figure 20.- Static longitudinal stability for several configurations and powers; center of gravity at 32-percent MAC.

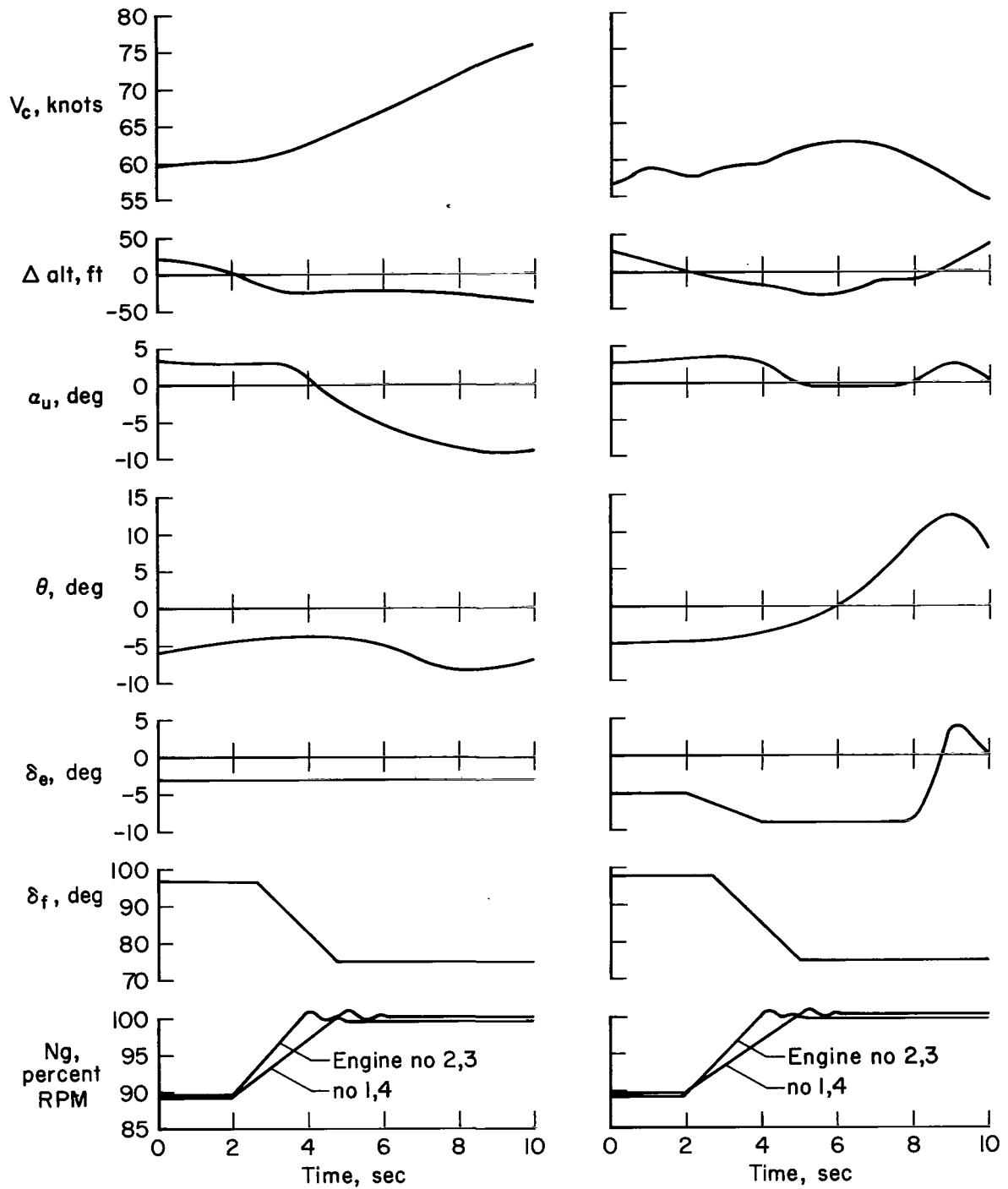


(a) Center of gravity at 35.2- and at approximately 30-percent MAC.



(b) Center of gravity at 30.8-percent MAC.

Figure 21.- Static longitudinal stability at various center-of-gravity positions.



(a) Without throttle-elevator interconnect.

(b) With throttle-elevator interconnect.

Figure 22.- Wave-off time histories with and without throttle-elevator interconnect;  $W = 36,800$  lb,  $i_t = 8.2^\circ$ , altitude  $\approx 6,500$  ft.

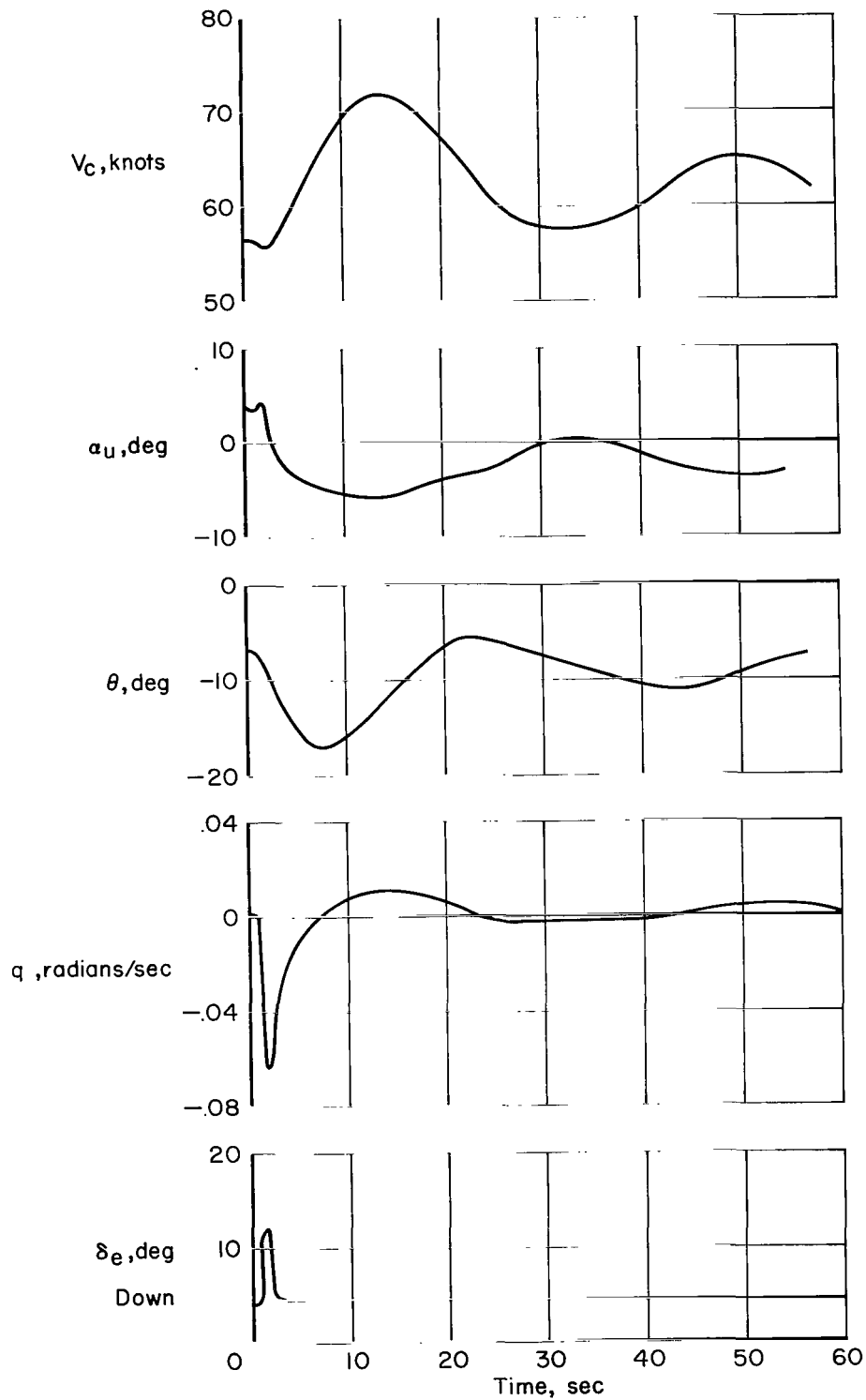


Figure 23.- Time history of an elevator pulse;  $\delta_f = 98/65$ , 700 shaft horsepower per engine,  $i_t = 9.0^\circ$ , center of gravity = 35.2-percent MAC.

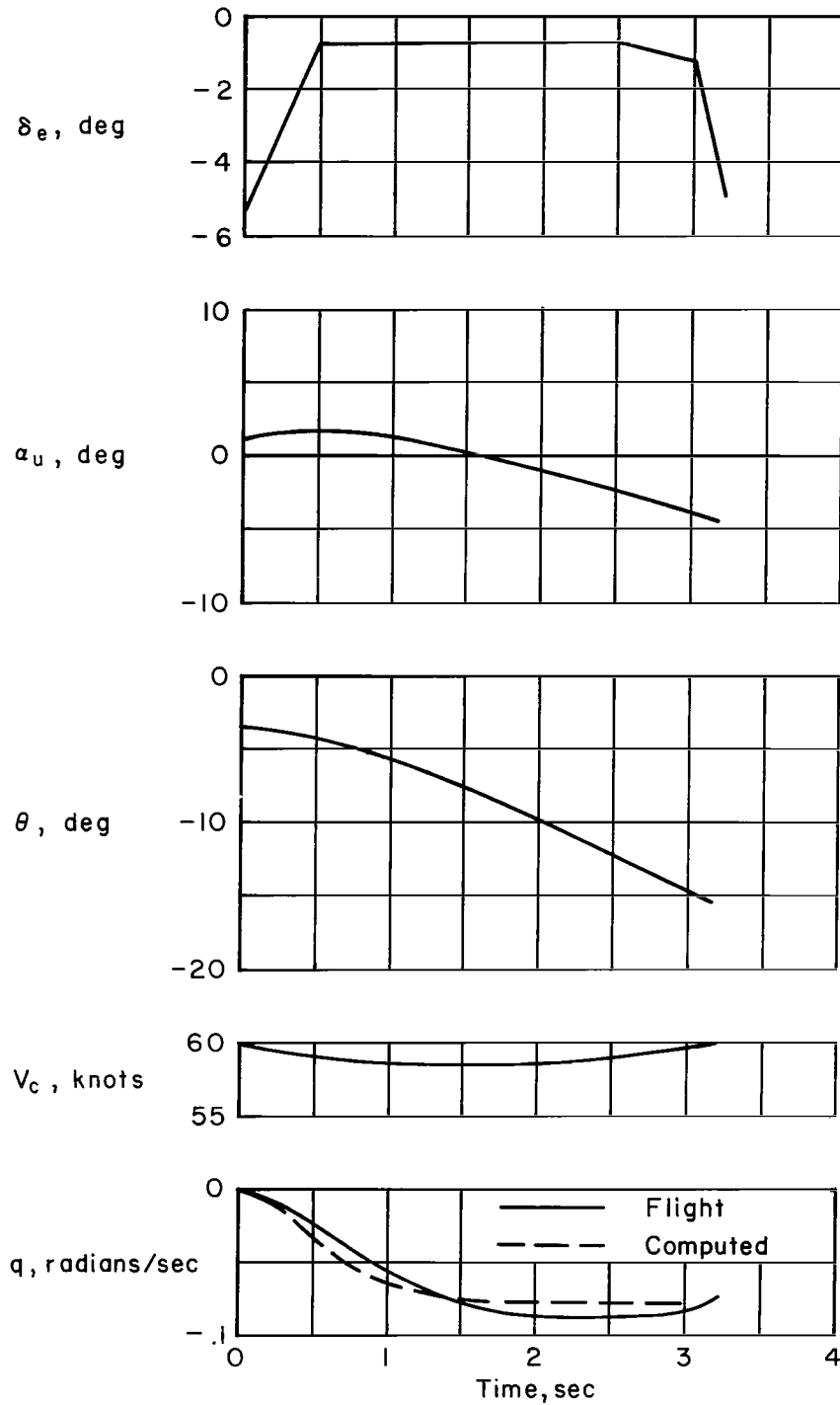


Figure 24.- Time history of elevator step;  $\delta_f = 98/65$ ;  
center of gravity = 30.8-percent MAC.

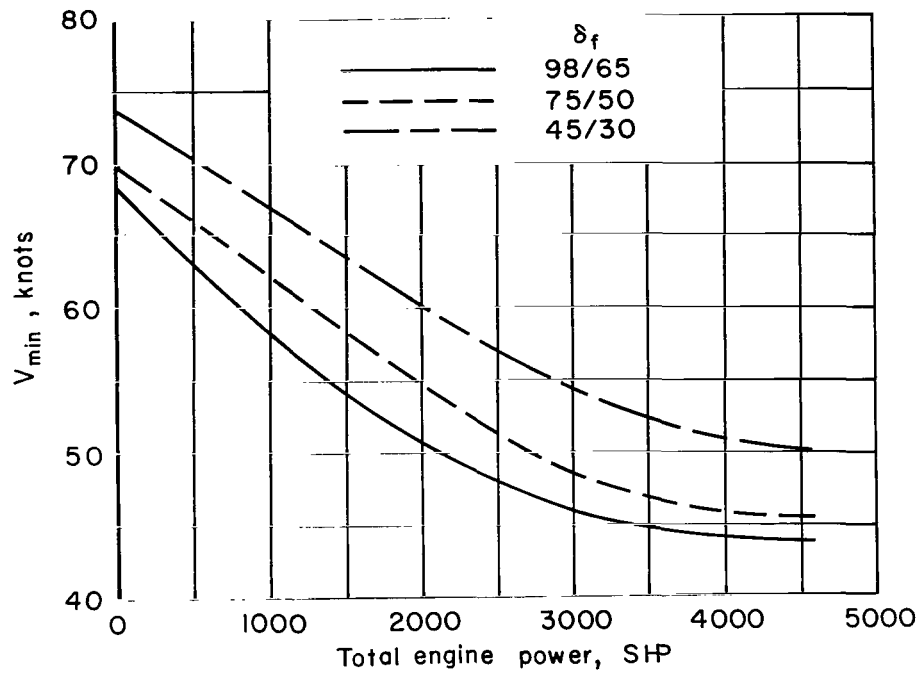


Figure 25.- Variation of minimum airspeed with engine power;  $W = 38,500$  lb.

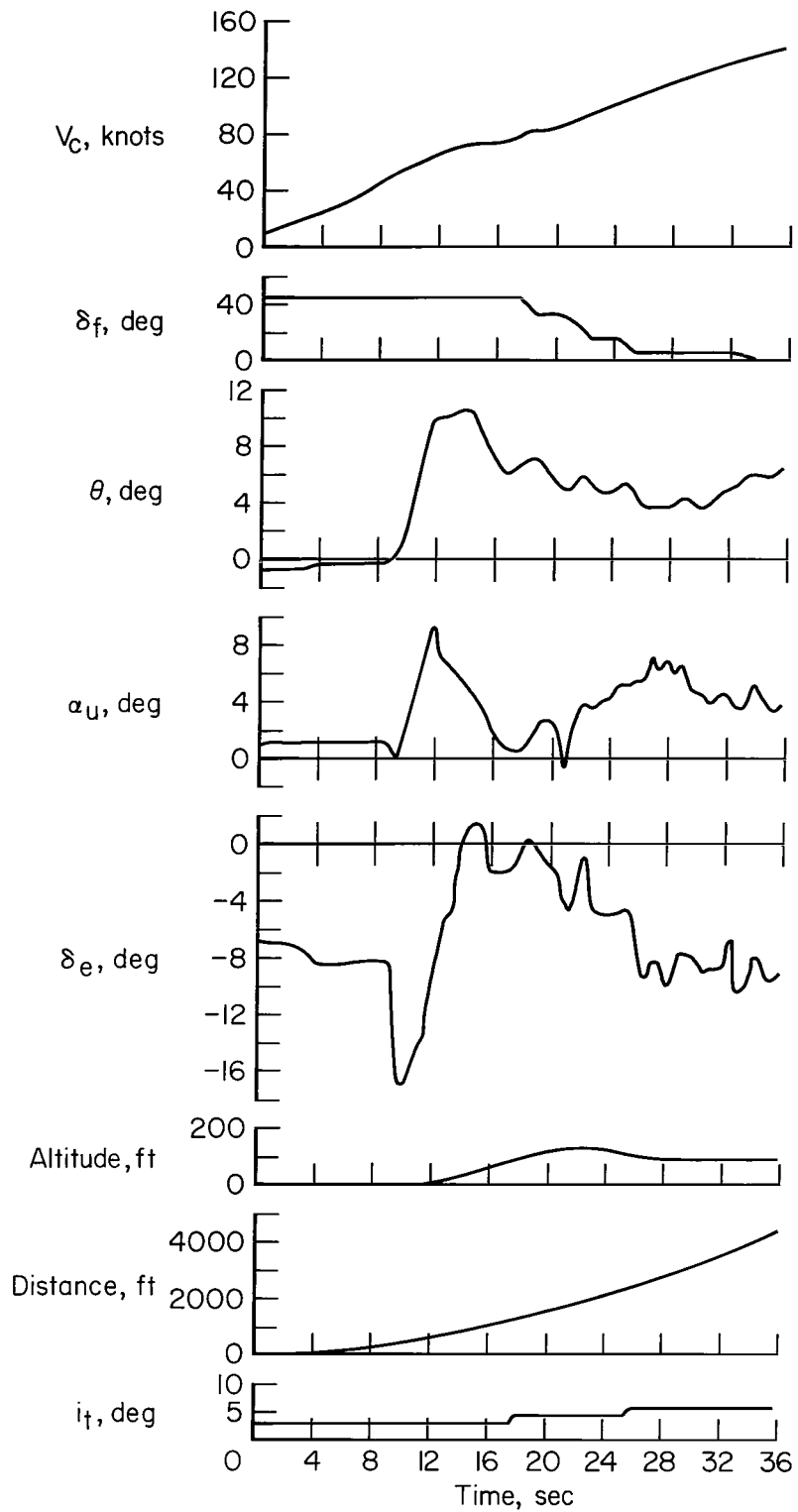


Figure 26.- Time history of take-off and transition to cruise.

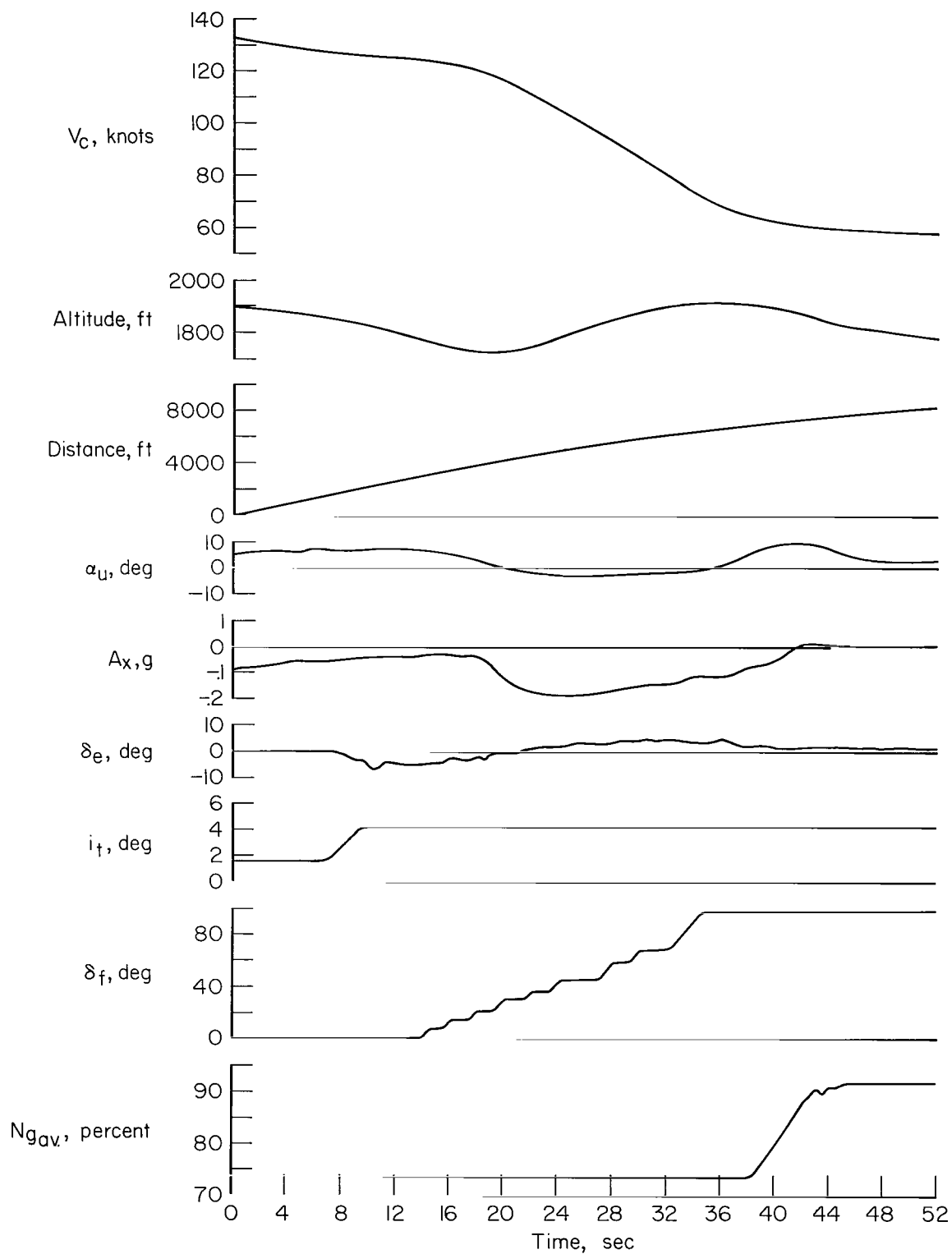


Figure 27.- Time history of transition from cruise to landing airspeed.

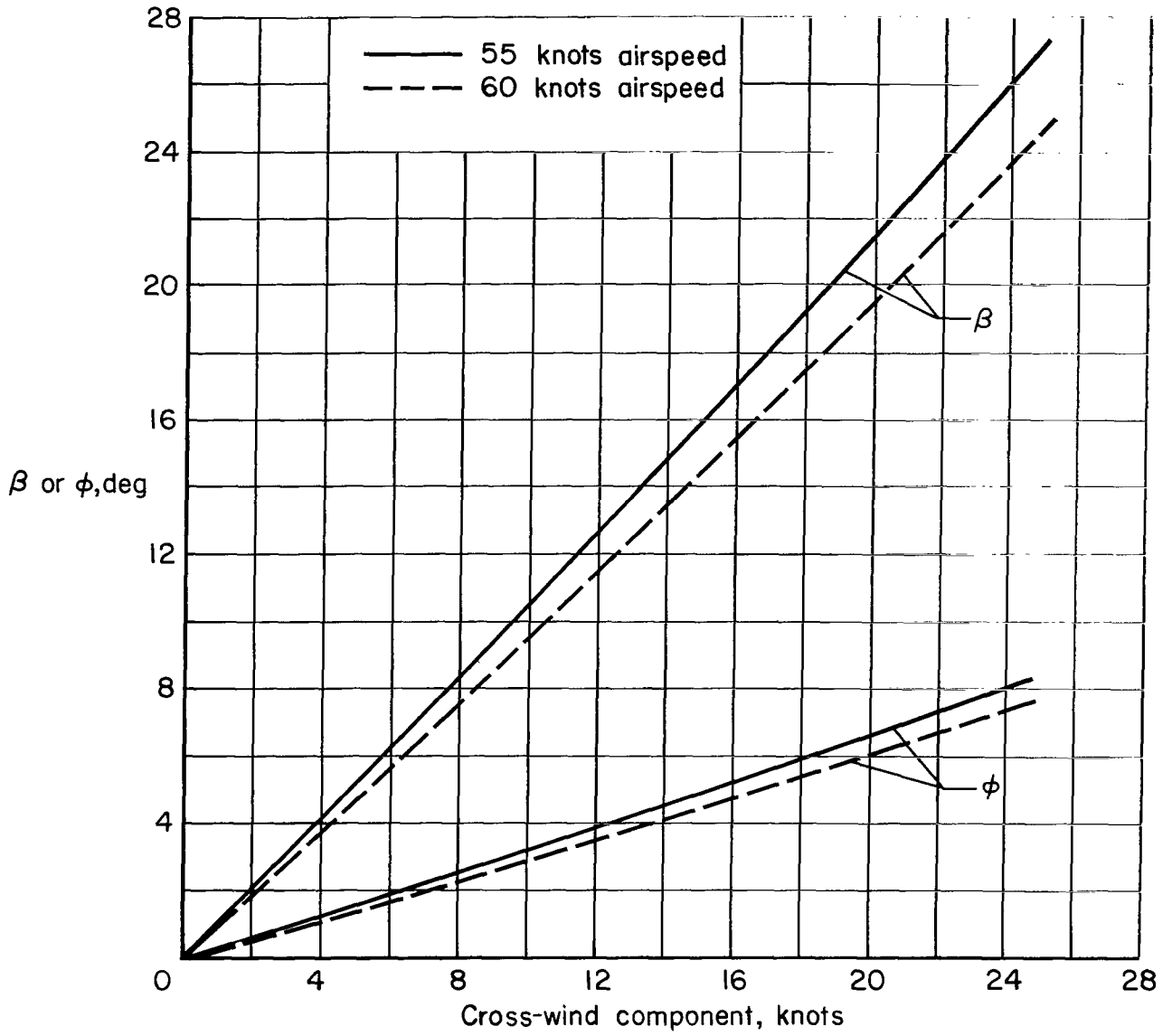
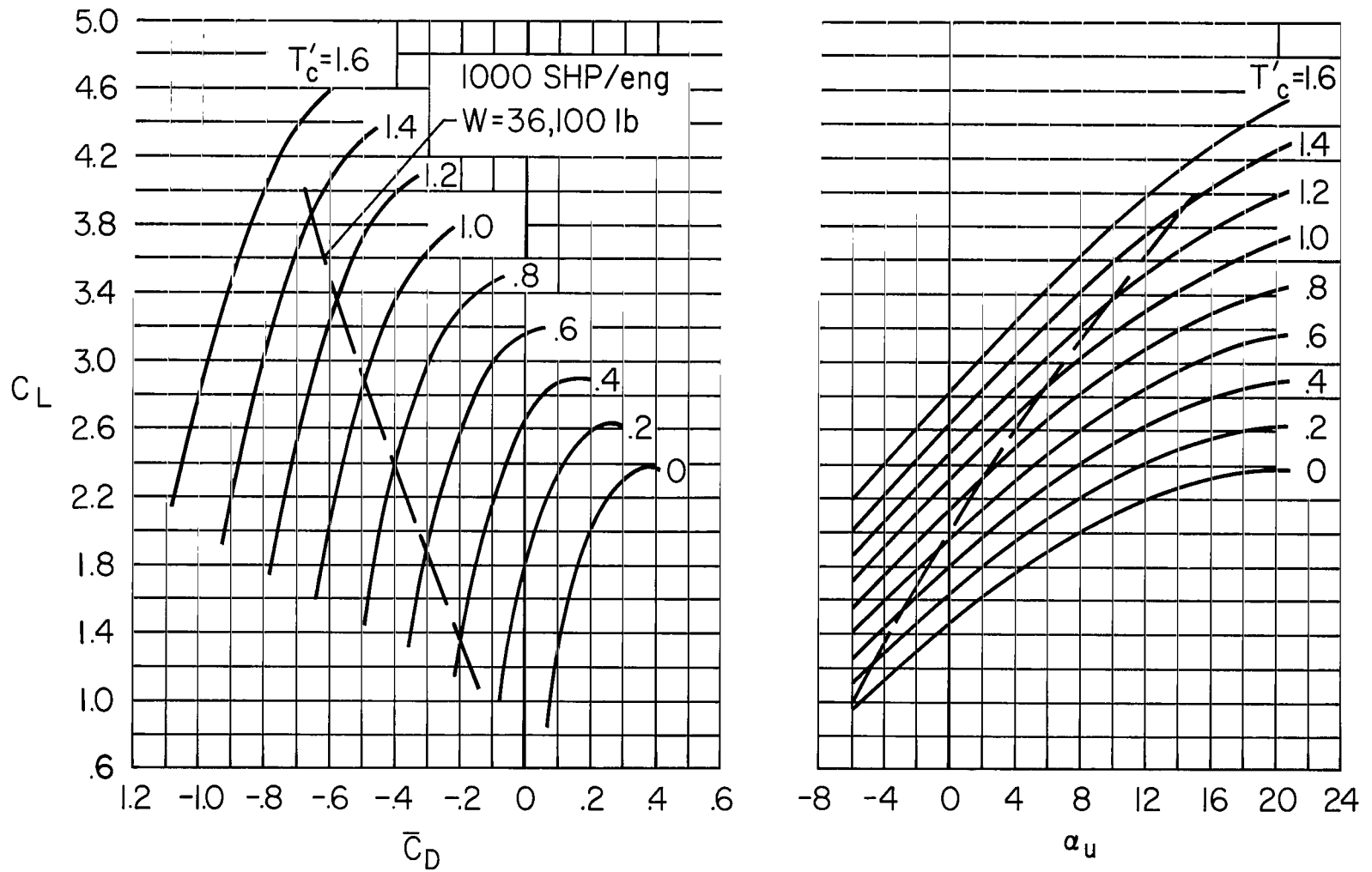
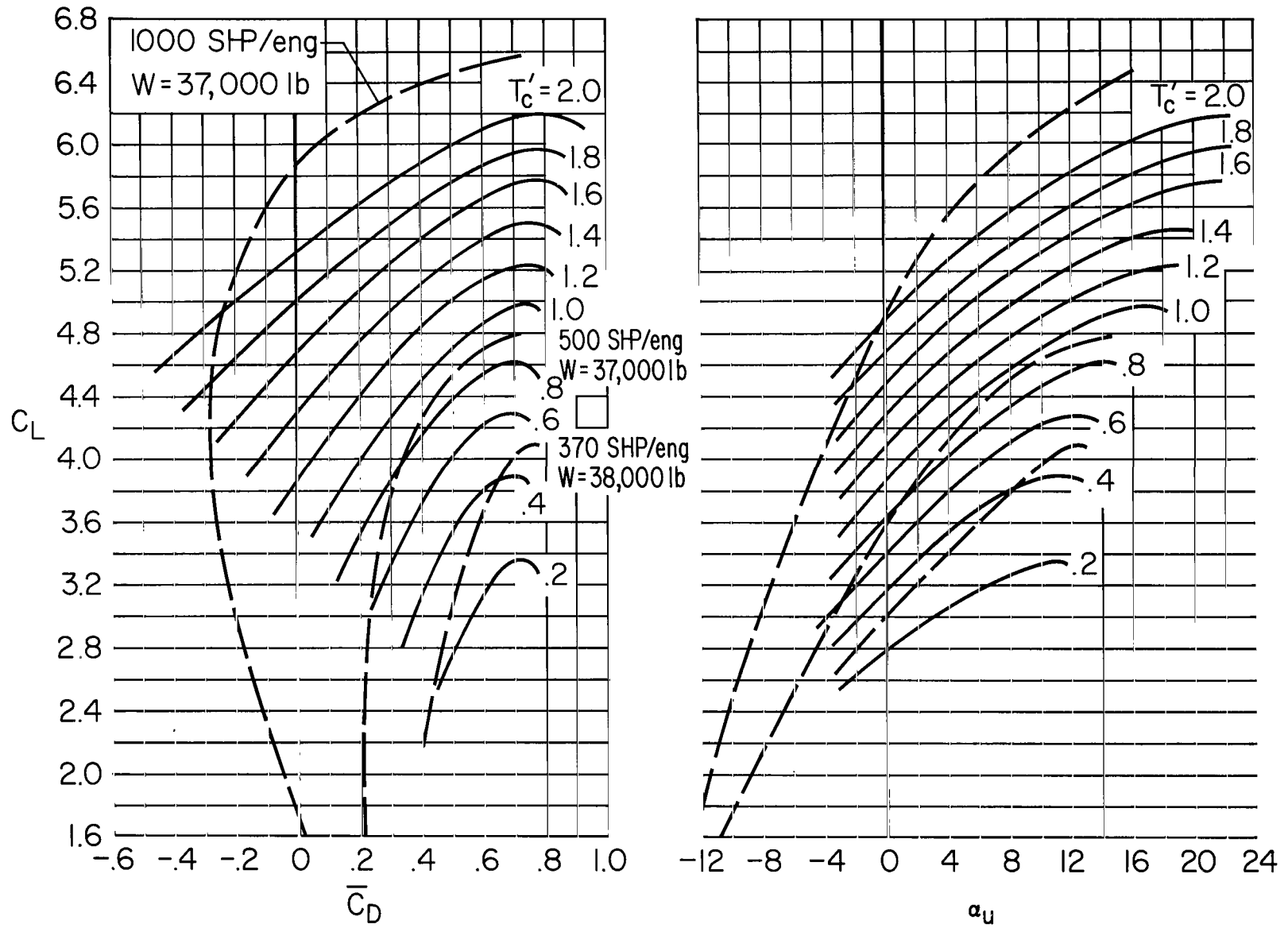


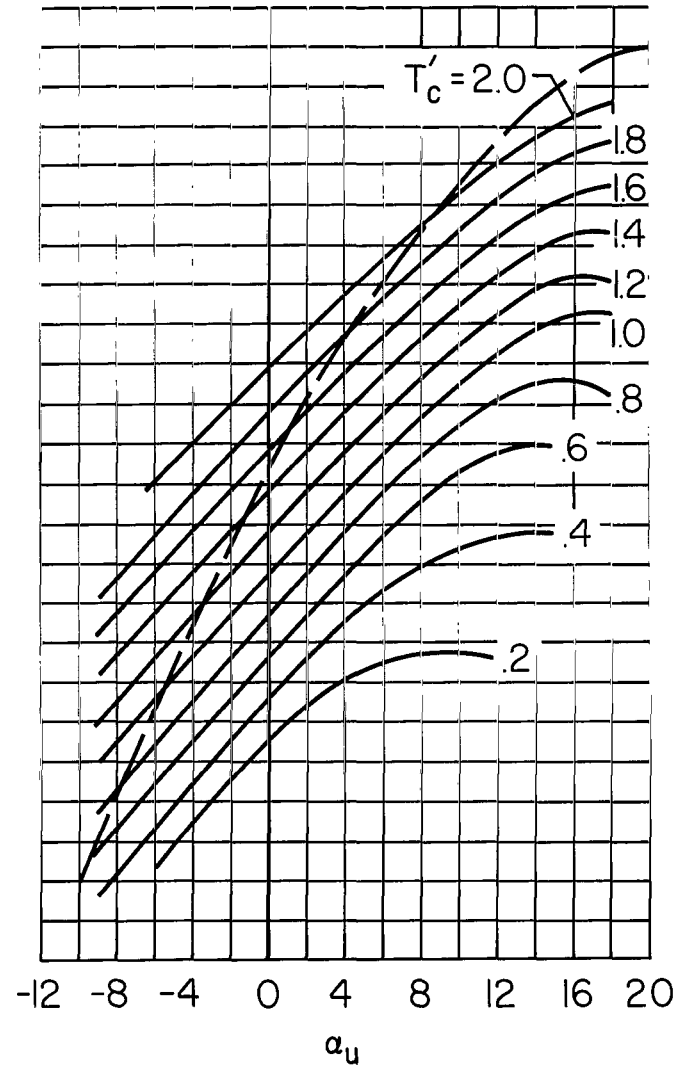
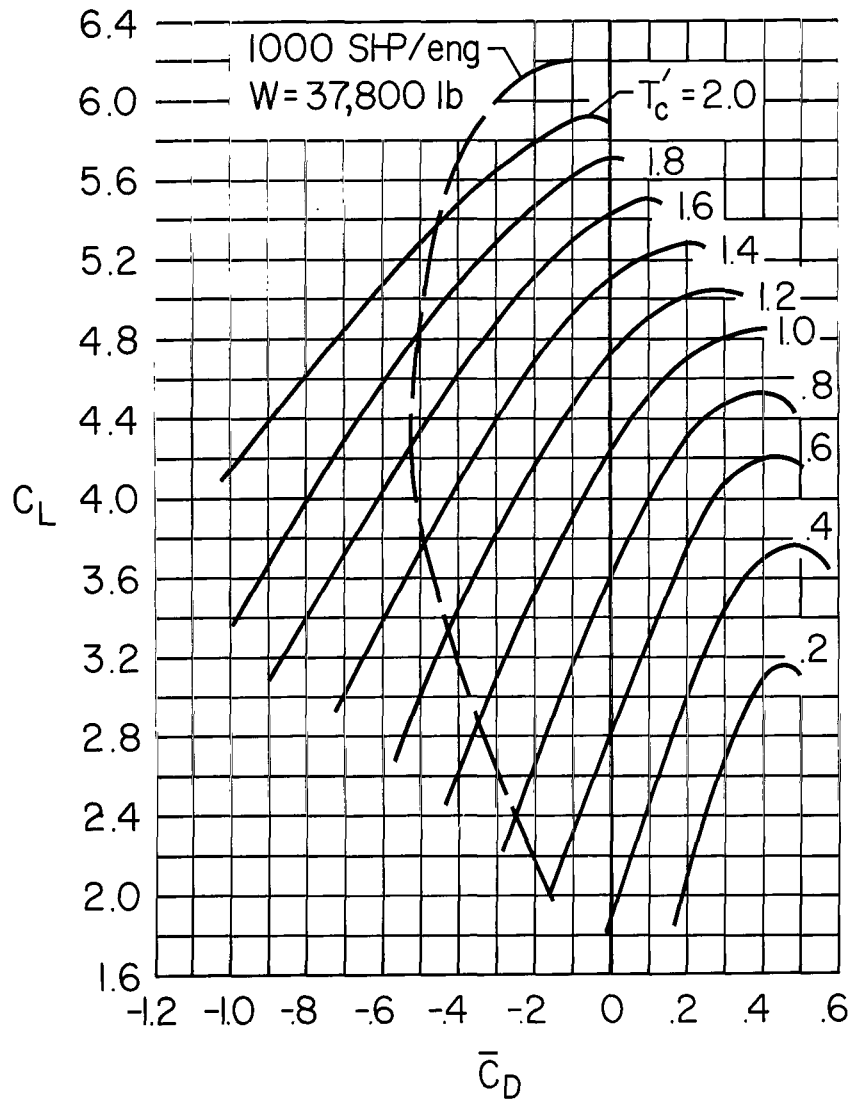
Figure 28.- Variation of sideslip and bank angle required to compensate for cross winds.



(a) Take-off configuration;  $\delta_f = 45/30$ .

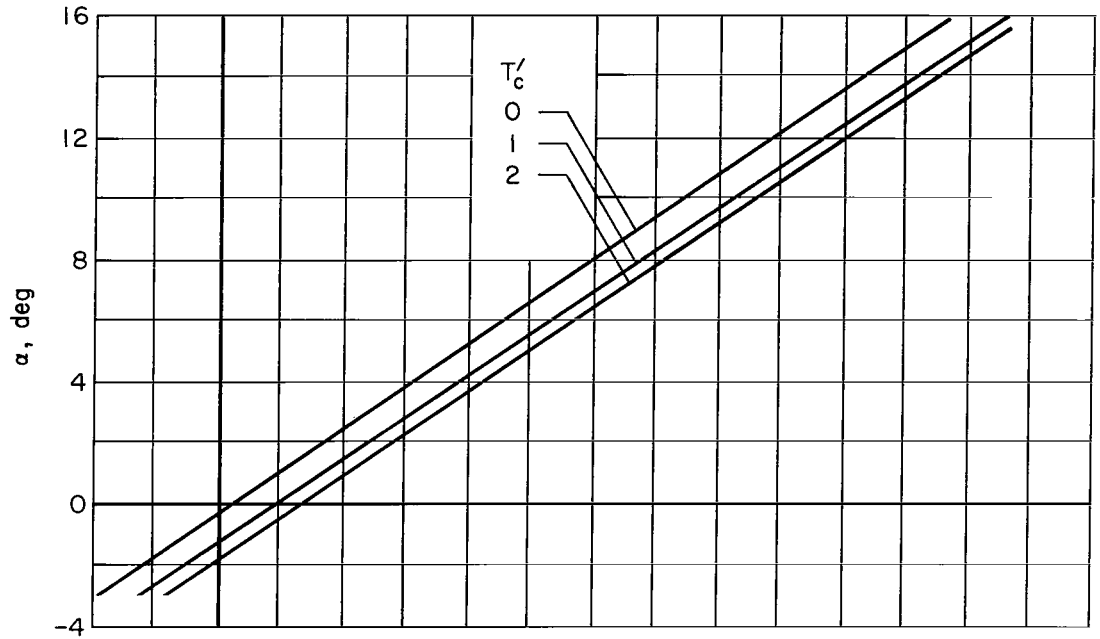
Figure 29.- Lift curve and drag polar variation with thrust coefficient.

(b) Landing configuration;  $\delta_F = 98/65$ .

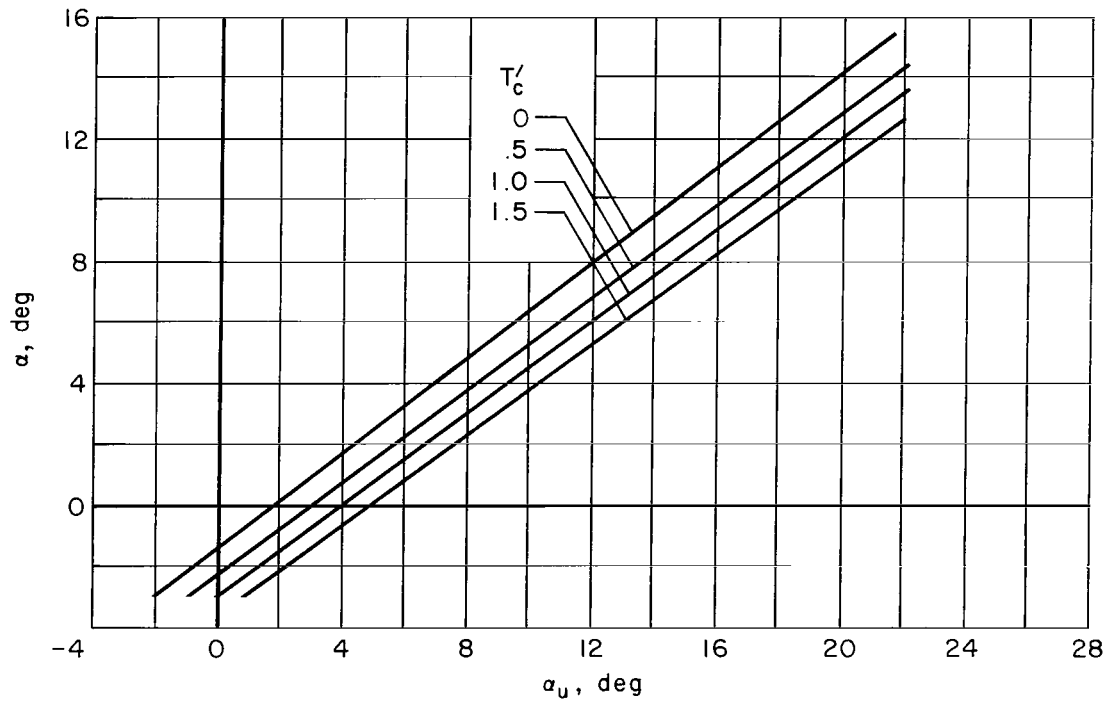


(c) Wave-off configuration;  $\delta_f = 75/50$ .

Figure 29.- Concluded.



(a) Take-off configuration.



(b) Landing configuration.

Figure 30.- Approximate angle-of-attack calibration.

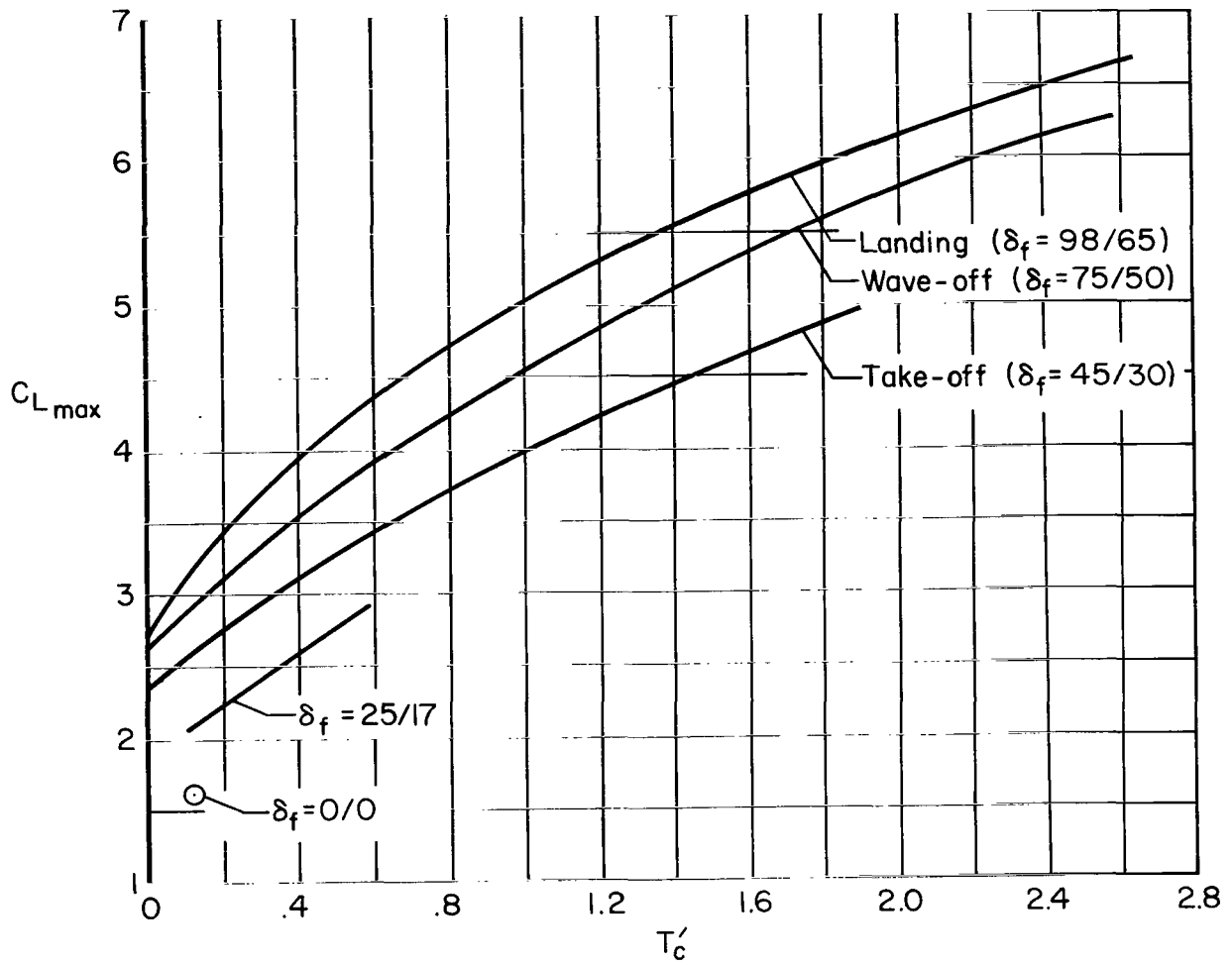


Figure 31.- Variation of  $C_{Lmax}$  with thrust coefficient for various flap configurations.

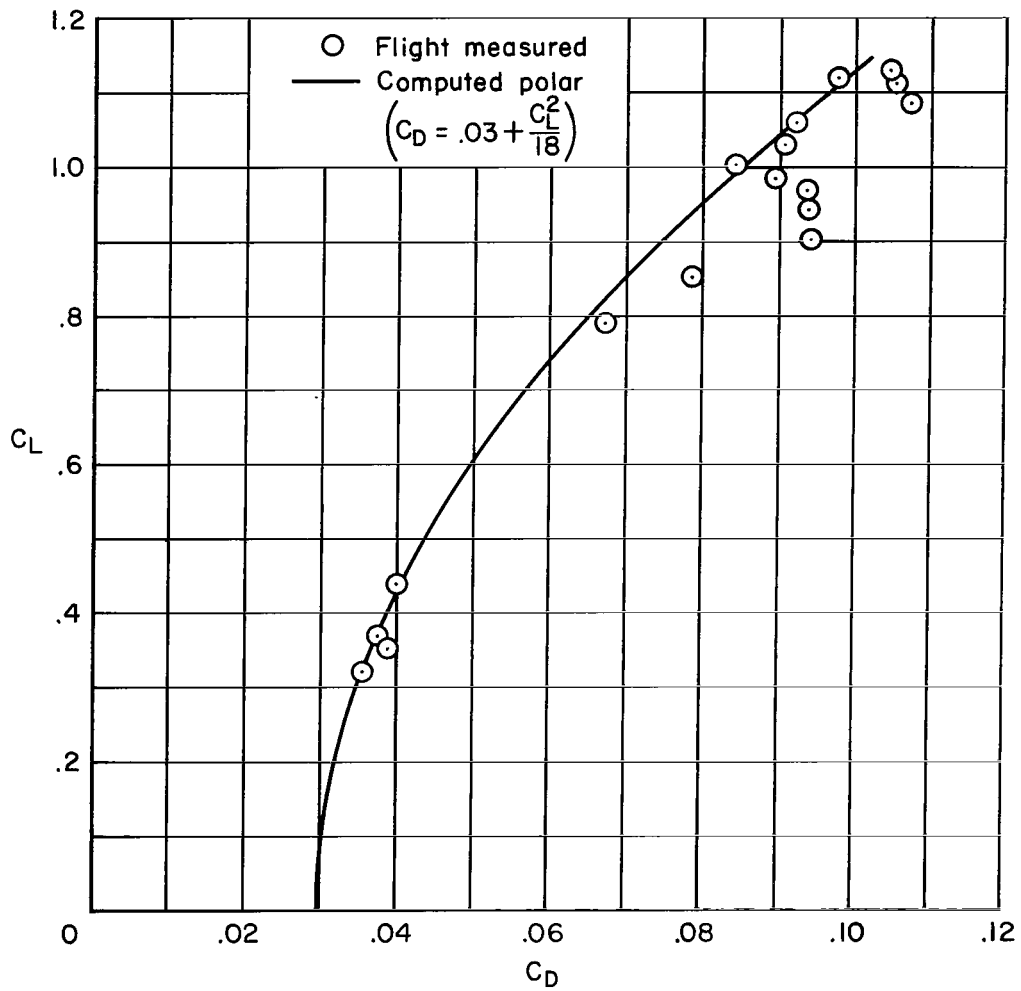


Figure 32.- Comparison between estimated drag polar and flight-test data;  
 $\delta_f = 0/0$ .